Draft Manuscript for Review

Controls of mantle potential temperature and lithospheric thickness on magmatism in the North Atlantic Igneous Province

Journal:	*Journal of Petrology*
Manuscript ID	JPET-Oct-15-0120.R1
Manuscript Type:	Original Manuscript
Date Submitted by the Author:	n/a
Complete List of Authors:	Hole, Malcolm; University of Aberdeen, Geology & Petroleum Geology Millett, John; VBPR AS
Keyword:	temperature, basalt, mantle plume, partial melting, P-T conditions

Controls of mantle potential temperature and lithospheric thickness on magmatism in the North Atlantic Igneous Province.

M. J. Hole[1]*, J.M. Millett[1,2]

[1]*Department of Geology & Petroleum Geology University of Aberdeen, AB24 3UE, Scotland*
[2]*Present address, VBPR AS, Forskningsparken, Gaustadalléen 21, N-0349 Oslo, Norway.*
**Corresponding author*

Modelled primary magma compositions of Palaeocene basalts from the North Atlantic Igneous Province (NAIP) require melting at mantle potential temperatures (T_P) in the range 1480-1550°C. Modern lavas from the Icelandic rift-zones required T_P~1500°C and those from the rift-flanks T_P~1450°C. Secular cooling of the NAIP thermal anomaly was therefore in the order of ~50°C in 61 Ma. There were systematic variations in T_P of 50-100°C from centre of the thermal anomaly to its margins at any one time, although limits on the stratigraphical distribution of T_P determinations do not rule out thermal pulsing on a timescale of millions of years. Variation in extent of melting at similar T_P was controlled by local variability in lithospheric thickness. In the west of the NAIP, lithosphere varied from ~90 km at Disko Island to ~ 65 km at Baffin Island, with similar thickness variations being evident for magmatism in the Faroe Islands, Faroe-Shetland Basin and the British Palaeogene Igneous Province (BPIP). Mean pressure of melting ≥ final pressure of melting and the two values converge for melting columns with a melting interval of < 1.5 GPa, regardless of T_P. In particular, the majority of BPIP magmas were mostly generated in the garnet-spinel transition in the upper-mantle. Calculated and observed rare earth element distributions in NAIP lavas are entirely consistent with the melting regimes derived from major element melting models. This allows a calibration of rare earth element fractionation and melting conditions that can be applied to other flood basalt provinces.

INTRODUCTION

The North Atlantic Igneous Province (NAIP; Fig. 1) is one of the best-known and most comprehensively studied Large Igneous Provinces on Earth. Two major phases of volcanism are recognised in the NAIP (Saunders *et al,*. 1997), the first beginning at ~62 Ma and largely restricted to western parts of the province (e.g. West Greenland, Baffin Island and the British Palaeogene Igneous Province), and the second and larger phase beginning at ~56 Ma focused more central to the site of NE Atlantic rifting (e.g. East Greenland and the Faroe Islands). Most models for magmatism in the NAIP require a thermal anomaly to have been present beneath the region from at least 61 Ma until the present day, the anomaly being ancestral to that responsible for present-day ridge-centred magmatism in Iceland. The evolution of the NAIP was controlled by the complex tectono-magmatic processes associated with the formation of rifted continental margins and the generation of new oceanic crust (Nielsen *et al.,* 2007; Hole *et al.,* 2015). Most plate reconstructions place the centre of the thermal anomaly beneath West Greenland at ~65 Ma, with an eastward migration over the next 20 Ma (Lawver & Müller, 1994; Milhaffy *et al.,* 2008). Over the period 64-58 Ma magmatism was widespread within the NAIP which has led to difficulties reconciling the distribution of magmatism with a simple 2000 km diameter thermal anomaly (e.g. Mihalffy *et al.,* 2008; Shorttle *et al.,* 2014; Hole *et al.,* 2015). Indeed, some magmatism in the British Palaeogene Igneous Province would have occurred at the very margins of the thermal anomaly and at the same time, near-primary picritic magmas were being emplaced in West Greenland and on Baffin Island.

Any study of magmatism associated with a thermal anomaly necessarily requires knowledge of mantle potential temperature (T_P). T_P expresses the mantle temperature projected along the solid-state adiabat to surface pressure. The MgO content of volatile-deficient primary magma generated by melting mantle peridotite is positively correlated with the temperature of the mantle. Based on this fundamental observation, Herzberg & Gazel (2009) demonstrated that the thermal anomalies that are responsible for melt generation in both ocean and continental large igneous provinces (LIPs) are of variable temperature and undergo secular cooling. In particular, Herzberg & Gazel (2009) proposed that the Icelandic plume required a very high cooling rate, from T_P = 1550-1650°C to values as low as 1460°C in a matter of 5 Ma. The record of magmatism for the Galápagos plume reveals two different cooling rates (Trela *et al.* 2015). The first occurred between ~90 and 70 Ma when T_P changed from ~1650 to 1550°C which was considered to represent the change from melting at the plume-head to that at the plume tail (Trela *et al*. 2015). From ~70 Ma to present time, the plume cooled from ~1550 to 1500°C (Trela *et al.,* 2015). Consequently estimates for the rate of secular change in T_P associated with LIPs vary considerably.

Because magmatism in the NAIP was geographically widespread as well as having longevity, the province potentially affords an opportunity to examine both spatial and temporal variations in T_P throughout the lifetime of a large igneous province. A number of existing studies have used a variety of different models to assess T_P at specific locations in the NAIP (e.g. Coogan *et al.,* 2014; Larsen & Pedersen, 2000; 2009; Scarrow & Cox, 1995; Scarrow *et al.,* 2000; Hole *et al*., 2015; Hole, 2015; Kerr *et al.,* 1999). Some T_P determinations have been made using olivine geothermometry (e.g. Larsen & Pedersen, 2000; 2009; Hole *et al.,* 2015), some using comparisons of major element data with experimental studies (Scarrow & Cox, 1995; Scarrow *et al.,* 2000) and others have relied on determining pressure of melting from the fractionation of rare earth elements (REE) and hence estimating T_P (e.g. Kerr *et al.,* 1999). Most recently, the petrological model PRIMELT of Herzberg & Asimow (2008) has been used to estimate T_P for picrites from Baffin Island in the extreme west of the NAIP and for parts of the British Palaeocene Igneous Province (BPIP) in the southeast of the NAIP (Hole, 2015; Hole *et al.,* 2015; Millett *et al,*. 2015).

Foulger (2012) highlighted the fact that methods for estimating mantle temperature suffer from ambiguity of interpretation with composition and partial melt, controversy regarding how they should be applied, lack of repeatability between studies using the same data, and insufficient precision to detect the 200–300°C temperature variations postulated. Here we present the results of a detailed study of the whole of the NAIP which includes the determination of T_P for 302 primitive basalts using the PRIMELT3 model of Herzberg & Asimow (2015). This single-model approach produces results that are internally consistent and can resolve T_P to ±42°C. We show that the results obtained agree well with those derived from some other, but not all, studies and conclude that the integration of the results from major element modelling with trace element variations provides a tool of great utility for the understanding the petrogenesis of flood basalts. The purpose of this study is not to debate the existence of mantle plumes, but to provide a new, internally consistent, T_P dataset for others to utilize in further debate.

STRATIGRAPHY AND AGE OF NAIP MAGMATISM

The relative and absolute ages of magmatism in the NAIP are based on an integration of isotopic ages, magnetostratigraphy and biostratigraphy (Fig. 2). Significant debate, however, still remains regarding the age of some parts of the NAIP due to conflicts between biostratigraphical and Ar-Ar / K-Ar isotopic age determinations for the commonly low K tholeiitic basaltic rocks of the main lava sequences (e.g. Passey & Jolley 2009; Cramer *et al.* 2013). The oldest lavas in the province are those of the 62.5-61 Ma Vaigat Formation (Larsen *et al.,* 2015) of Baffin Island and West Greenland (mainly Disko Island; Fig.1). Magmatism was continuous in West Greenland from 62-58Ma, followed by a magmatic hiatus at 56-58 Ma followed by continued magmatism from 56 until 53 Ma (Larsen *et al.,* 2015). The age of British Palaeogene Igneous Province (BPIP; Fig. 1b) volcanic rocks is constrained by cross-cutting relationships with dated intrusive rocks and interbedded acid lavas (Hamilton *et al*., 1998; Chambers & Pringle, 2001; Ganerød *et al.,* 2010). The Tardree Rhyolite Complex in Northern Ireland gives a U-Pb zircon age of 61.32±0.09 Ma and sits between the Lower and Upper Basalt Formations of the Antrim Lava Group. The Skye Main Lava Series (SMLS) is younger than the Rum layered igneous complex (60.53±0.08 Ma) but is intruded by the Cuillin gabbro (zircon U-Pb age of 58.91±0.07 Ma). The Mull Plateau Lava Formation (MPLF) is cut by the Loch Ba Ring Dyke (58.12±0.13 Ma; Chambers & Pringle, 2001) a best-estimate for extrusion of the MPLF being ~60.5 Ma, although biostratigraphical constraints suggest a rather younger age for the MPLF (~55 Ma; Jolley & Bell, 1997). The Faroe Island Basalts Group (FIBG) spans the Palaeocene-Eocene Thermal Maximum (PETM; 55.8 Ma), with the stratigraphically oldest Lopra and Beinisvørð formations being pre-break-up and the stratigraphically younger Malinstindur and Enni formations being syn-break-up, which are comparable with the ages determined for Geike Plateau and Milne Land formations of East Greenland (Larsen *et al.*, 1999; 2009; Peat *et al.,* 2008; Passey & Jolley, 2009). Overall, the NAIP lavas under consideration here span ~5-8 Ma of stratigraphy. In addition, at ~60-61 Ma, lavas are distributed over a wide geographical area in relationship to the position of the proposed plume centre.

CALCULATION OF PRIMARY MAGMA COMPOSITIONS

The model PRIMELT3 and the associated macro MEGAPRIMELT (Herzberg & Asimow, 2015) both of which are derivatives of PRIMELT2 (Herzberg & Asimow, 2008) and PRIMELT (Herzberg & O'Hara, 2002), has been used here to generate primary magma compositions from major element data on lavas. Hereafter this will be referred to as simply PRIMELT. PRIMELT software uses a mass balance solution to the primary magma problem calibrated to fertile peridotite KR-4003, derived from a parameterization of experimentally determined partial melt compositions (Herzberg & O'Hara, 2002; Herzberg, 2004a; 2004b; 2006; Walter, 1998). PRIMELT uses both forward and inverse modelling to constrain a unique solution for primary magma composition. This is achieved by computing a melt fraction that is common to both partial melts of mantle peridotite and to the primitive magmas from which the lava in question was derived (Herzberg & Asimow, 2008; 2015). In this way, it differs from other methods that use olivine composition to constrain primary magma composition (e.g. Lee *et al.* 2009; Putirka, 2008; Putirka *et al.,* 2007; Courtier *et al.*, 2007). Critical aspects of the PRIMELT model are that melts must have had olivine as the sole liquidus phase during crystallization and melt must have been derived from volatile-deficient peridotite. Melts which show evidence of early augite crystallization can be effectively identified by the use of covariations between MgO and CaO, because augite causes significant fractionation of CaO relative to MgO, but olivine does not, and the data set used here has been filtered accordingly. In addition, T_P information cannot be obtained for melts derived from pyroxenite sources within the upper mantle, and such samples are identified because of their deficiency in CaO for a given MgO content compared to melts from mantle peridotite. PRIMELT contains an algorithm that identifies such samples (Herzberg & Asimow, 2015; 2008).

Construction of adiabatic P-T pathways and estimates of T_P

For primitive basalts that have crystallized only olivine, reverse-modelling involving the incremental addition or subtraction of equilibrium olivine to the measured bulk-rock composition allows the generation of a suite of potential parental melt compositions (Herzberg *et al.,* 2007). A model parental magma is defined by the coincidence of an olivine addition array with a ‘target’ olivine phenocryst composition having the maximum Fo content (Herzberg & Asimow, 2008). Comparison of parental melts compositions with primary melt compositions determined from forward models of peridotite melting, allows T_P that is required to generate the melt to be estimated (Herzberg & Asimow, 2008). The initial pressure of intersection of the dry peridotite solidus (*Pi*) can be determined from T_P. Since the MgO content of an accumulated fractional melt does not change substantially as melt fraction increases during decompression, the adiabatic temperature–pressure melting path is nearly coincident with the olivine liquidus such that the P-T pathway of the primary melt to the surface can be simulated. Fig. 3 is a schematic pressure-temperature diagram illustrating the relationships between the principal parameters that are derived during the generation of a modelled primary magma composition using PRIMELT. The example used is Vaigat Formation olivine-phyric basalt BI/CS/8 from Baffin Island (Starkey *et al*. 2009) which has a whole-rock content of 9.7 wt% MgO. PRIMELT calculates the primary magma to this basalt to contain 19.0 wt% MgO, (27.6% olivine addition to the analysed composition) which requires T_P=1540°C. The intersection of the dry peridotite solidus and the 1540°C adiabat gives the initial pressure of melting P*i* = 4.2 GPa at T ~ 1620°C (Fig. 3).

Effects of variations in peridotite composition on T_P.

The MgO and FeO contents of KR-4003 are two of the fundamental values from which all other PRIMELT parameters are derived. Decreasing the FeO/MgO of the mantle peridotite source composition, which can be achieved by melt extraction (depletion), will give higher T_P than that for models derived from KR-4003. To examine the magnitude of these effects, we have calculated the compositions of residues after melt extraction from KR-4003 of natural samples covering a range of T_P = 1360-1600°C and *F-AFM* ~0 to 0.3, using equation (9) of Herzberg & Asimow (2015). Detailed descriptions of these estimates are given in Electronic Appendix 1, which may be downloaded from the Journal of Petrology Web site at http://www.petrology.oupjournals.org. Estimates were only made for SiO_2, FeO, MgO and CaO since KR4003 is somewhat deficient in TiO_2 and Na_2O and high in K_2O, and P_2O_5 compared to typical peridotites of similar fertility (Herzberg & Asimow, 2015). The MgO and FeO content of the various residues derived has then been used as the MgO and FeO content of the peridotite source for PRIMELT, and sample BI/CS/8 has then been remodelled using the melt residue values as the peridotite source. An increase in T_P of ~ 100°C is achieved for a decrease in FeO/MgO of the peridotite source from ~0.211 to ~0.174. This is equivalent to the depletion achieved in the residue from fertile peridotite KR-4003 after extraction of a melt similar in composition to that being produced today at Mauna Kea. Such depletion is considered unlikely in nature, and in addition, the low CaO content of the residue would render the peridotite of low fertility. An increase in T_P of ~ 50°C is achieved for FeO/MgO = 0.19 which is a similar to the composition of depleted abyssal peridotite RC27-9-30 (Baker & Beckett, 1999; Herzberg & O'Hara, 2002). Detailed discussions on the choice of the peridotite source for PRIMELT are given elsewhere (e.g. Herzberg & O'Hara, 2002) and here we wish to acknowledge the fact variability in the composition of mantle peridotite can affect T_P values and other petrological parameters used in this study.

Melt fraction, final pressure of melting and mean pressure of melting

Mantle peridotite partially melts at low melt fractions to produce melt droplets that are efficiently removed from the residue by buoyancy-driven draining. During decompression melting, the melt droplets mix to produce an "aggregate" or accumulated fractional melt (*AFM*). The melt fraction (*F-AFM)* is uniquely defined by the MgO and FeO contents of any accumulated fractional melt. It does not depend on the temperatures and pressures at which melting begins and ends, and applies to all polybaric and isobaric accumulated fractional melting paths (Herzberg & O'Hara, 2002). However, in nature mantle peridotite melts progressively during decompression along an adiabatic T-P path, generating accumulated fractional melts with lower FeO at nearly constant MgO. The final melting pressure (P*f*), which represents the pressure at which the last drop of melt was produced, can be estimated from the melt fraction and P*i*. The precise method for determining P*f* is dependent on both the composition of the primary magma and the range of pressures under consideration. Details of the calculation methods used here are given in Electronic Appendix 2. For sample

BI/CS/8, P*f* = 1.9 GPa (Fig. 4) which corresponds to *F-AFM* ~ 0.3 at a temperature of 1520°C along the 19.0 wt% MgO isopleth (Fig. 3). P*f* is also useful because it allows the total depth of the melting column to be estimated and gives the approximate depth of lithosphere–asthenosphere boundary (Gazel *et al.*, 2011). However, complex phase transitions at high pressures limit P*f* estimates to ≤ 3.5 GPa (Herzberg & Gazel, 2009).

Lee *et al.* (2009) provided a magma thermo-barometer for calculating the average pressure and temperature of melt segregation from the mantle for primary magma compositions (here referred to as P*m*). Calculation of P*m* is based on the silica activity in olivine and orthopyroxene saturated melts (Lee *et al.,* 2009) and gives the mean pressure of melting over the depth of a melting column with an uncertainty of ±0.2 GPa. P*m* is therefore is always ≥ P*f* and is comparable to the mean pressure of melting described by other workers (e.g. Klein & Langmuir, 1987; Albarède, 1992; Hole & Saunders, 1996). Here, we have calculated P*m* from primary magma compositions derived from the PRIMELT model for which P*f* is therefore also available. For sample BI/CS/8 (Fig, 3) the Lee *et al.* (2009) geo-barometer indicates P*m* ~ 2.6 GPa compared to P*f* = 1.9 GPa. Continued rise of the parental magma to BI/CS/8 to pressures lower than 1.9 GPa occurred along the olivine liquidus and was accompanied by ~28% olivine crystallization but without further melting.

Residual mantle mineralogy

The three residual mantle mineralogies that are predicted by PRIMELT are garnet peridotite or spinel peridotite or harzburgite. These residues are the solid that was left behind, not the solid in equilibrium with the aggregate primary melt. The residue must therefore have a mineralogy that reflects the final pressure of melting for the primary magma in question. Lithology of the residue is predicted using a molecular projection of primary magma compositions onto the plane Ol-An-Qz from or towards diopside which has three compositional fields representing spinel peridotite, garnet peridotite and harzburgite residues

(Fig. 4). For any primary magma, P*f* must be within the pressure-temperature range for the stability of the aluminous phase (spinel or garnet) in the residue. The exhaustion of clinopyroxene during melting of mantle peridotite is dependent on *F-AFM* ('cpx-out' line in Fig. 3) and represents the transition from a spinel peridotite residue to a harzburgite residue. Inspection of Figs 3 and 4 shows that for BI/CS/8 initial melting took place within the garnet stability field of the upper-mantle, and then for P*f* = 3.1-2.9 GPa in the garnet-spinel transition, and finally in the spinel stability field of the upper-mantle. Harzburgite was the residual lithology for the final drop of melt at P*f* = 1.9 GPa (Fig. 4). However, the mean pressure of melting for BI/CS/8 (P*m* = 2.6 GPa) is within the spinel stability field of the upper mantle.

Melting of volatile-bearing peridotite

Mantle peridtotite that contains H_2O or CO_2 or both, melts at lower temperatures than volatile deficient ('dry') peridotite of the same silicate major element composition at the same pressure (e.g. Dasgupta *et al.,* 2007; Metrich *et al.,* 2014). Melting in the presence of CO_2 drives primary magma compositions towards more silica under-saturated compositions with higher CaO than for melting of dry peridotite (Dasgupta *et al*., 2007). PRIMELT utilizes this information in an algorithm that satisfactorily identifies primary magmas derived from peridotite with >~0.5 wt% CO_2 (Herzberg & Asimow 2008) and such compositions have been discounted in this study. For H_2O-bearing peridotite an appropriate algorithm cannot be derived principally because of a lack of suitable data. However, Jamtveit *et al.* (2001) reported water content of olivine from a number of volcanic rocks from the NAIP, including Vaigat Formation picrites and basalts from the Faroe Islands, all of which had H_2O contents that were below detectable limits (< 0.5 wt%). East Greenland lavas with determinable levels of H_2O in olivine, indicative of > 300 ppm H_2O in the mantle source (Jamtveit *et al.*, 2001), are mostly silica under-saturated compositions (alkali picrite and nephelenite) which do not yield PRIMELT solutions. Nichols *et al.* (2002) reported values of 620-920 ppm for the mantle source of basalts beneath Iceland, but these estimates were dependent on the degree of melting assumed (Nichols *et al.* 2002). However there are no full major element analyses for these samples and so their significance cannot be assessed here. In a more general context, Peslier and Bizmis (2015) showed that the bulk water content of Hawaiian peridotite xenoliths is 50-100 ppm and Adria *et al.* (2012) concluded that hydrous partial melting cannot occur at 4.5-7.5 GPa for H_2O concentrations in the range 50–200 ppm, which are typical of the convecting upper-mantle sampled by mid-ocean ridge basalts (MORB). While we cannot totally discount a role for H_2O-bearing peridotite in the generation of NAIP primary magmas based on the currently available data, for the remainder of this study, we make the assumption that melting occurred under anhydrous conditions.

Crustal contamination

Because the rocks making up the continental crust in the area of the NAIP are of considerable antiquity, they have characteristically unradiogenic Nd- and Pb-isotopic compositions with the most contaminated basalts having εNd_T = -30 and $^{206}Pb/^{204}Pb$ = 14.3 (Thompson *et al.,* 1986; Dickin *et al.,* 1987; Saunders *et al.,* 1997; Fowler *et al.,* 2003). Additionally, because primitive magmas of the NAIP have low REE abundances, any interaction with crust readily moves magma compositions to unradiogenic Nd-isotopic compositions (e.g. Skye Main Lava Series and Mull Plateau Lava Formation εNd_T as low as -30; Thompson *et al*., 1986; Dickin *et al.,* 1987; Thompson & Morrison, 1988. Vaigat Formation εNd_T ~ -21 and $^{206}Pb/^{204}Pb$ ~15.5; Larsen & Pedersen 2009). For West Greenland lavas, the majority which have unradiogenic Nd-isotopic compositions (εNd_T -20.0 to 0.0) are quartz-normative basalts which do not provide PRIMELT solutions; indeed no *Qz*-normative NAIP basalts provide solutions for primary magmas by this method. For the NAIP data set used in this study, all samples which yield primary magma solutions and for which Nd-isotopic compositions are

277 available (44 in all) have εNd_T >4.0 and 38 samples have εNd_T >6.0. In addition, elevation of key trace element ratios above values expected for the upper-mantle can also be used to identify possible crustal interaction (e.g. La/Nb, Th/Nb, Ba/Zr; Thompson *et al.,* 1982; Kent & Fitton, 2000; Hole *et al.,* 2015). Where such data are available, we again find that all samples which yield primary magma solutions carry no evidence of interaction with continental crust. This is perhaps not surprising since addition of partial melts of fusible crust to a mantle-derived mafic magma will cause phase changes which will mean that inverse modelling to a parental and primary magmas is unlikely to succeed. Consequently, it seems that the PRIMELT model satisfactorily identifies samples that have undergone significant crustal interaction and does not provide a primary magma solution for them.

RESULTS FOR THE NAIP

Data sources and model parameters

Published data that were generated from previous versions of PRIMELT have been recalculated to the new dry peridotite solidus parameters of Herzberg & Asimow (2015). Data were taken from the GEOROC database, with total iron recalculated to FeO where necessary. Samples with ≥ 8.5 wt% MgO were used to minimize complex fractionation effects at lower contents of MgO. The majority of samples used were olivine tholeiites which exhibit early iron enrichment, and it has therefore been assumed that Fe_2O_3/TiO_2=0.5. Whilst some basalts from the Vaigat Formation are *Ne*-normative alkali olivine basalts, Fe_2O_3/TiO_2 has also been set to 0.5 because *Ne* makes up <5% of the norm. Results obtained from PRIMELT are summarized in Table 1 and illustrated in Figs 5-8. For individual stratigraphical units, or in some cases, geographical regions, mean values of T_P, P*i*, P*f* and *F-AFM* are given (Table 1) and the uncertainty is quoted at 2 standard deviations (2σ) on the mean of the population. The internal uncertainty in T_P determination by PRIMELT is approximately ± 30°C and that for P*i*, P*m* and P*f* ± 0.3 GPa (Herzberg & Asimow, 2008; Lee *et al.,* 2009). P*m* was calculated from the PRIMELT primary magma solutions using the method of Lee *et al.* (2009). Results for geographical and stratigraphical subdivisions of the NAIP will be considered in turn below. In all cases, PRIMELT3 results refer to the locus of magma generation, which for some areas (e.g. BPIP) is not necessarily the locus of final magma emplacement (Hole *et al.,* 2015). The full dataset of PRIMELT3 solutions is given in Electronic Appendix 4.

Vaigat and Maligat formations (West Greenland and Baffin Island).

Vaigat Formation lavas from Disko and Baffin islands provided 126 PRIMELT solutions with T_P varying from 1496 to 1639°C. Seven samples from Disko Island yield T_P 1606-1639°C requiring initial intersection of the dry peridotite solidus at 5.9-7.1 GPa (Fig. 4). These samples form a distinct group in Fig. 4 and have FeO contents > 0.5 wt% higher than all other Vaigat Formation basalts. The remaining 119 Vaigat Formation lavas have a normal distribution of T_P with 99.7% of samples falling within 2σ (38°C) of the mean of 1541°C and with a median value of 1544°C. We consider T_P ~ 1540°C to be the best estimate for Vaigat Formation magmatism. Melting ceased at < 2.0 GPa and melt fractions produced were in the range F = 0.10 to 0.32, with the mean melt fraction being 0.26 ± 0.06. There is no evidence of any stratigraphical variation in melting regime within the Vaigat Formation, and similarly there are no differences in melting regimes for the N-type and E-type magmas described by Dale *et al.* (2009) and Starkey *et al.* (2009). However, there are significant differences in the melting regimes at Baffin Island compared to Disko Island. For Baffin Island lavas, the residual lithology was spinel peridotite, or harzburgite with only four samples having garnet peridotite as the residual lithology (Fig. 4). P*m* beneath Baffin Island was 2.8 ± 0.8 GPa which for T_P = 1530°C requires the majority of melt to have been formed in the spinel stability field of the upper-mantle. By contrast, at Disko Island, garnet peridotite was the residual lithology for 51 primary magmas, spinel peridotite for 25 primary magmas and harzburgite for only four primary magmas. P*m* (3.5 ± 1.2 GPa) requires most melt to have been formed in the garnet stability field of the upper-mantle beneath Disko Island. Differences in T_P and P*i* between the two locations are not large enough to explain the differences in residual mineralogy between the two locations. Consequently P*f* and by inference lithospheric thickness was the dominant control of extent of melting for the Vaigat Formation. Two samples from the overlying Maligat Formation yielded PRIMELT solutions with T_P = 1511 and 1527°C.

East Greenland

Results for East Greenland are little different from those reported by Herzberg & Gazel (2009). 19 samples provided solutions for melting of dry peridotite, 4 of which yielded T_P =1640-1650, 14 yielded T_P in the range 1508-1568°C and the remaining 5 samples yielded T_P = 1444-1468°C. Eight samples from the Milne Land Formation (Fig. 1) have T_P 1528-1568°C which overlaps with the range of data for Vaigat Formation lavas. The lower temperature group from East Greenland comprises basalts from the Hold With Hope succession (Fig. 1) and two samples from the seaward-dipping reflector sequences sampled during ODP Leg 152. Melt fractions produced were in the range F = 0.14 to 0.28. The mean melt fraction was 0.27±0.08 for the higher T_P samples and 0.20±0.06 for the lower T_P samples. The residual lithology for East Greenland primary magmas was spinel peridotite or harzburgite

British Palaeogene Igneous Province (BPIP)

49 samples from the BPIP yielded PRIMELT solutions, all of them from the regional dyke swarm of the BPIP. Data have a normal distribution of T_P with 99.7% of samples falling within 2σ (65°C) of the mean of 1504°C and with a median value of 1506°C. T_P variations within the BPIP are therefore greater than the uncertainty of T_P determinations by PRIMELT, although we cannot distinguish any systematic stratigraphical or geographical variation in T_P.

Extents of melting were variable (F = 0.04-0.27; mean = 0.16 ± 0.08) which is reflected in the large range of Pf (1.3-3.4 GPa). However, 43 out of 49 solutions gave Pf >3.5 – 2.5 GPa. Pm (2.9 ± 0.8 GPa) is within error of Pf. 35 samples had a garnet peridotite residue, the remainder a spinel peridotite residue. Melt inclusions in olivine phenocrysts from two MPLF lava flows (Peate *et al.,* 2012) have been treated in the same way as whole-rock data. Six inclusions yielded PRIMELT solutions that suggest T_P = 1455-1482°C (Fig. 5). As an independent assessment of the validity of using the PRIMELT model on melt inclusion data, major element data for 23 melt inclusions from olivine phenocrysts in Vaigat Formation picrites from Baffin Island (Yaxley *et al.,* 2004) were processed, and these yielded T_P = 1533±22°C (Electronic Appendix 4) which is within the range for Vaigat Formation whole-rock samples from the same location (T_P = 1532±48°C).

Faroe Island Basalt Group (FIBG)

34 samples from the Enni and Malinstindur formations of the FIBG provided PRIMELT solutions and data have a normal distribution of T_P with 99.7% of samples falling within 2σ (36°C) of the mean of 1519°C and with a median value of 1520°C. No samples from the Beinisvørð or Lopra formations, both of which stratigraphically underlie the Malinstindur Formation (Fig. 2), yielded PRIMELT solutions. There are no distinctions between the Malinstindur and Enni formations of the FIBG in terms of melting regime. Extents of melting are greater for the FIBG (F = 0.22 ± 0.06) compared to the BPIP (F = 0.16 ± 0.04), a function of melting to lower pressures in the FIBG (Pf < 2.4 GPa) rather than variation in T_P and thus Pi. The residual lithology for FIBG primary magmas was spinel peridotite or harzburgite.

Modern Iceland

Icelandic lavas have been divided into two groups based on their geographical relationship to the major rift-zones. Rift-zone magmatism is represented by lavas that were emplaced along the continuation of the MAR on land, in the western (WVZ) and northern (NVZ) volcanic zones (Peate *et al.,* 2010; Hardarson *et al.,* 1997). Volcanism occurs on the rift-flanks at Snaefell and Snæfellsnes. Snæfell represents the site of incipient rifting above the fringe of the plume, and Snæfellsnes is situated on an old transform (Hards *et al.,* 2000; Mattsson & Oskarsson, 2005). 41 rift-flank lavas gave T_P = 1455±28°C (Table 1; Fig. 8) whereas 56 lavas from the rift-zones gave T_P = 1504±26°C. The value of T_P~1450°C for the rift-flanks is in agreement with the estimates given by Herzberg & Gazel (2009), but the higher T_P of ~1500°C for the rift-zones is previously unreported. This establishes that there is a T_P gradient across modern Iceland which occurs on a scale of hundreds of km. For both rift-zone and rift-flank magmatism there are large variations in P*f* (1.4 – 3.0 GPa). However, because of T_P variations, extents of melting are larger in the rift-zones (*F* = 0.17-0.30) than on the rift-flanks (*F* = 0.13-0.21) which is a consequence of the higher P*i* for the rift-zones (3.2-4.1 GPa) than the rift flanks (2.7-3.2 GPa). There is no discernible difference in the mean pressure of melting for the rift zones (2.6±0.6 GPa) and for the rift-flanks (2.3±0.6 GPa).

DISCUSSION

Mantle potential temperature variations in the NAIP

Ambient mantle T_P is considered here to be that which is required to generate ocean ridge basalts, which is ~ 1350°C (Herzberg *et al.,* 2007; Herzberg & Gazel, 2009; Hole, 2015; Lee *et al.* 2009). Whilst there is limited evidence to suggest T_P > 1600°C for some Disko Island lavas, the majority of > 55 Ma NAIP magmatism appears to have driven by a thermal anomaly of ambient mantle T_P +200°C that is ~1550°. This is similar to T_P for Hawaii at present-day (T_P = 1540 ± 20°C), slightly higher than that required for the generation of basalts from the Ontong Java Plateau (T_P = 1524 ± 5°C) and the Etendeka Province of southwestern Africa (T_P = 1515 ± 16°C) and considerably higher than that for many ocean island basalts (Herzberg & Asimow, 2008; Herzberg & Gazel, 2009; Gazel *et al.,* 2011; Hole, 2015). In general, there are three distinct distributions of T_P in the NAIP (Figs 6 and 7). Firstly, Vaigat Formation and Milne Land Formation lavas required T_P ~1550°C. Secondly, BPIP, FIBG and Iceland rift zone lavas all have very similar distributions of T_P (1500-1510°C) which is ~40-50°C lower than for Vaigat Formation lavas. Finally, Iceland rift-flank lavas required T_P ~ 1450°C. As a statistical exercise, the combined T_P values for Iceland Rift Zones, the BPIP and FIBG give T_P = 1509±48°C and for the Vaigat Formation and Milne Land Formation combined T_P = 1541±38°C. A student's *t*-test (*t* = 4.31) shows that the difference in these mean values is significant at the 99% confidence level. Consequently, we identify three T_P regimes during magmatism in the NAIP over the period 62-0 Ma, corresponding to T_P = 1550°C, 1500°C and 1450°C.

Modern Iceland

Herzberg & Gazel (2009) argued that the Iceland plume underwent significant secular cooling from the Palaeocene (T_P~1550°C) to the present (T_P~1450°C) whereas Herzberg & Asimow (2015) derived T_P=1500°C from samples from the Western Rift-zone. The latter T_P is in good agreement with the rift-zone results presented here, and we therefore suggest that secular cooling for the Iceland plume has been around 50°C in 55 Ma. Evidence suggests that since 55 Ma, the Iceland plume has produced pulses of hotter than average material (+ 25-30°C) that expanded radially at up to 40cmyr^{-1}, with periods of low magma productivity represented by troughs between V-shaped ridges on the Reykjanes spreading Ridge (Parnell-Turner *et al.,* 2013; 2014; Poore *et al.,* 2009; Hardarson *et al.,* 1997). The possibility therefore remains that the rift-zone T_P of ~1500°C represents the beginning of one such pulse, and that the rift-flank T_P of 1450°C represents the 'background' plume temperature. There is also an additional possible role for H_2O in the source-region of Icelandic basalts that cannot be dismissed (Nichols *et al.* 2002). However, the key point is that for modern Iceland the assumption of a steady-state T_P~1450°C is not valid. Therefore T_P fluctuations of at least ±50°C in the magmatic record of the NAIP might be expected.

Palaeocene-Eocene lavas

Within the older (> 50 Ma) sequences of the NAIP there are some clear indicators of variations in T_P in time and space (Fig. 6). Magmatism was initiated in West Greenland and on Baffin Island, on either side of the Davis Strait at ~ 61 Ma (Fig. 1). Whilst there is evidence to suggest T_P up to 1640°C at this time, 90% of T_P determinations (a total of 119) are in the range 1496-1600°C with a mean value of T_P = 1541±38°C. Two samples from the SDRS on the East Greenland margin, which are considered to be near age-equivalents of the Vaigat Formation lavas (Larsen *et al.*, 2015), give T_P = 1453 and 1461°C, suggesting a change in T_P of ~100°C from West to East at ~60-61 Ma. Basalts from the ~55 Ma Milne Land Formation at Blosseville Kyst (Larsen *et al.,* 2014; Waight *et al.,* 2012) farther north along the East Greenland margin (Fig. 1), give T_P~1540°C. It is generally accepted that by 55 Ma the location of the plume centre had migrated to the east, to a position under central Greenland. The T_P values obtained from the Milne Land Formation basalts are consistent with this hypothesis. Five samples from Upper Plateau Lava Series basalts from Hold With Hope (Fig. 1) give T_P = 1485-1561°C, and whereas these values are more variable, they are not inconsistent with the relocation of the plume centre at that time.

FIBG lavas from the Malinstindur and Enni formations record T_P ~ 1519±36°C (Fig. 6) ~ 30°C lower than for Vaigat Formation lavas. The Malinstindur and Enni Formations were both emplaced during the syn-rift phase of Larsen *et al.* (1999), and are thought to have been located 100-200 km to the south of the Central East Greenland succession at that time. The pre-break-up lavas of the Faroe Islands (Lopra and Beinisvørð formations; Passey & Jolley, 2009), which represent over 4 km of stratigraphy, underwent augite ± plagioclase fractionation and available samples do not yield PRIMELT solutions. However, the lower-most lavas from well 217/15-1 in the Faroe-Shetland basin are likely to be correlatives of the Beinisvørð Formation of the FIBG (Millett *et al.* 2015) and these yielded T_P~1530°C. However, there are insufficient data to allow resolution of stratigraphical T_P variations within the FIBG, because T_P variations are close to the uncertainty in T_P determinations using PRIMELT.

T_P data obtained from BPIP whole-rocks (T_P = 1504±64°C) is restricted to samples from the Preshal More and Central Mull formations which mostly occur in the regional dyke swarm of the BPIP (Hole *et al.,* 2015). These results suggest that BPIP magmatism took place at $T_P \leq$ 1510°C, whereas melt inclusion data suggest that the plateau-forming lavas resulted from melting at T_P~1480°C, which is consistent with estimates of Scarrow & Cox (1995). If the majority of the BPIP required $T_P <$ 1510°C, this value is lower than that for both the younger (FIBG and East Greenland) and older (West Greenland) sequences to the north. The exception is for the few slightly older Leg 152 SDRS samples which give cooler temperatures. There is little doubt that the BPIP was on the periphery of the plume system at ~60-61 Ma (Fig. 1; Mihalffy *et al.,* 2007; Hole *et al.,* 2015) and it seems reasonable to suggest that the distance of the BPIP from the plume head resulted in a smaller T_P anomaly than above the plume head itself. Certainly, the fact that the rare earth element distributions in many BPIP plateau lavas had residual garnet in their mantle source requires a minimum T_P of ~1475°C (Thompson *et al.,* 1986; Kerr *et al*., 1999; Hole *et al.,* 2015). However, it is also apparent that a linear decrease in temperature with distance from the proposed plume head during the Palaeogene is not supported by all the data. We conclude that at present, there is no evidence to suggest that T_P was > 1510°C beneath the BPIP at ≤ 61 Ma.

Comparisons with other temperature estimates for the NAIP

Larsen & Pedersen (2000) calculated primitive melt compositions for magnesian lavas from Disko Island by stepwise addition of equilibrium olivine to the composition of the glassy matrix of pillow lavas. Calculated primitive magmas had 20-21wt% MgO and liquidus temperatures of 1515-1560°C at 1.4-1.6 GPa. Temperatures and pressures of primary magma segregation were 1563-1606°C and 2.8-3.6 GPa respectively. Recalculating segregation temperatures to T_P gives 1538-1559°C, values which are in excellent agreement with T_P from PRIMELT. Other T_P estimates for the NAIP as a whole, based on a wide range of different methods and assumptions (e.g. Gill *et al.,* 1992; Scarrow *et al.,* 2000), give T_P = 1420-1600°C depending on the model applied. Maclennan *et al.* (2001) derived T_P=1480-1520°C for modern Iceland based on REE inversion modelling and crustal accretion rates at Herdubreid in the NVZ of Iceland. Herdubreid samples HBT1 to HBT5 (Appendix 3) yield PRIMELT solutions with T_P=1487-1498°C. Parnell-Turner *et al.* (2014) used an average excess Iceland plume temperature of ambient T_P = 150±50°C in a study of transient mantle plume activity beneath Iceland from 55 Ma to present-day, a range which is greater than that given by PRIMELT solutions. However Howell *et al.* (2014) showed that for ambient T_P=1338 °C, and an Iceland plume with T_P=1488 °C (ambient +150 °C), a thermal anomaly of ≥ 55°C (1393 °C) would extend to 1000 km from the plume-head position. If the plume was hotter during the Palaeocene with T_P = 1540°C, as indicated by Vaigat Formation lavas, then it may have been possible to produce absolute T_P≥1500°C 1000 km from the plume centre, assuming the plume position of Mihalffy *et al.* (2007). This would have been sufficient to support the generation all NAIP magmas to the east of West Greenland, particularly if the plume-head migrated eastwards through time.

Pressure of melting and lithospheric structure.

P*f* is influenced by the thickness of the lithosphere above the site of melting and may be used as a proxy for the depth to the lithosphere-asthenosphere boundary (LAB; Gazel *et al.*, 2011). P*m* is based on the silica activity in olivine and orthopyroxene saturated melts and reflects the mean extent of melting over the depth of the melting column (Klein & Langmuir, 1987; Albaréde, 1991; Hole & Saunders, 1996; Lee *et al.,* 2009). Whilst P*f* must be within the pressure-temperature range for the stability of the aluminous phase (spinel or garnet) in the residue, P*m* is frequently higher than that indicated by the residual mineralogy from melting. Thus for Vaigat Formation lavas from Baffin Island, P*f* indicates pressures lower than the garnet-spinel transition in the upper mantle, but P*m* straddles the transition (Fig. 8). A similar distribution of P*f* and P*m* is also exhibited by FIBG and Iceland rift-zone lavas. Using a combination of P*i*, P*m* and P*f*, the average dimensions of melting columns for any location at any T_P can be estimated (Fig. 9). Values of P*f* represented in Fig. 9 are the mean P*f* of primary magmas with the lowest pressure residual lithology i.e. spinel peridotite or harzburgite or both of these, for the locations in question. It is assumed that melting columns are cylindrical which is a simplification because plumes are likely to deform as they impact the base of the lithosphere (e.g. Saunders *et al*., 1997; Herzberg & Asimow, 2015).

For Siqueiros MORB, P*f* ≈ P*m* ≈ 1.4 GPa (Fig. 9) indicating a depth of 50 km to the base of the LAB, equivalent to ~25 Myr old lithosphere (Lee, 2005). For the Ontong-Java Plateau, P*f* ≈ 1.7 GPa indicating a depth of 55 km to the LAB with a mean pressure of melting of ~2.5 GPa. Ontong-Java Plateau lavas were therefore mostly generated in the spinel stability field of the upper-mantle, with extensive melting (*F* ~ 0.3) leaving a harzburgite reside. For Icelandic rift-zones, magmas leaving a harzburgite residue, which are commonest at Theistareykir, require P*f* ~ 1.5 GPa with the LAB at ~ 50 km. Icelandic rift-flank magmas have more consistent and higher P*f* ~2.1 GPa (~ 65 km) compared to the rift-zone primary magmas, but have a lower T_P and P*i*, and hence represent smaller melt fractions than rift-zone primary magmas. The lithosphere thicknesses for Iceland derived here are therefore similar to other estimates (e.g. the summary given by Barnhoorn *et al.,* 2011).

At Baffin Island, the LAB was at ~ 65 km depth and P*m* (~ 2.8 GPa) was within the spinel stability field of the upper mantle. The melting column for Disko Island was truncated at ~ 2.8 GPa representing a cap of ~ 90 km of overlying lithosphere. P*m* ~ 3.3 GPa requires melting beneath Disko Island to have occurred in the presence of garnet, which is consistent with the residual lithologies derived from PRIMELT. These observations are in good agreement with those of Larsen & Pedersen (2009) who argued for lithosphere ~100 km thick at Disko Island. This also implies that the LAB was at least 30 km thinner beneath Baffin Island than Disko Island at 61 Ma. Palaeocene oceanic crust within palaeomagnetic chron 27r, which ends at 62.0 Ma (Larsen *et al.,* 2009) is present in the Davis Strait (Fig. 1). The oldest Palaeocene volcanic rocks dated from the region are tholeiitic basalts dredged from the Davis Strait High with an $^{40}Ar/^{39}Ar$ age of 63.0±0.7 Ma (Larsen *et al.,* 2009). The geochemistry of these basalts indicates formation beneath a strongly attenuated continental lithospheric lid (Larsen *et al.,* 2009). Therefore, it is proposed that before the onset of magmatism on Baffin Island, the lithosphere was already significantly thinned, allowing for extensive decompression melting. Farther to the NE at Disko Island, it can be assumed that the continental crust was still at its pre-stretching thickness resulting in a TBL thickness >100km.

The melting column for FIBG primary magmas is similar in its dimensions to that for Baffin Island, but T_P (~ 1520°C) and P*i* (~ 3.9 GPa) are a little lower than those for Baffin Island. The mean P*f* values for the FIBG (~ 2.1 GPa) requires the LAB to have been at a depth of ~ 65 km at the time of generation of the Enni and Malinstindur formations lavas. Farther to the south, in the Faroe-Shetland Basin (Fig. 1), basalts from the base of the lava pile in well 217/15-1 have P*f* ~ 3.0 (T_P ~ 1530°C), which requires the base of the lithopshere to be ~ 30 km deeper than beneath the Faroe Islands. The age of the lavas in 214/15-1 is not well constrained and consequently their relationship with break-up is not well-understood. However the 217/15-1 lavas are likely to be equivalent to the Beinisvørð Formation of the FIBG (Millett *et al.* 2015) and therefore may pre-date break-up. Whatever the age of the

217/15-1 lavas, they provide evidence for significant fluctuations in the thickness of the lithosphere in the Faroe Islands and Faroe-Shetland Basin area during NAIP magmatism, and suggest that the lithosphere was thinned before magmas forming the Malinstindur and Enni formations were generated.

Beneath the BPIP, the depth to the LAB was similar to that for Disko Island (~ 2.7 GPa or ~ 90 km). However, since the samples which yield PRIMELT solutions are from the regional dyke swarm of the BPIP, it is likely that they were emplaced at some distance from the site of melting (Hole *et al.,* 2015). Nevertheless, this depth estimate is consistent with previous estimates based on distributions of the REE (Thompson, 1982; Kerr *et al.*, 1999; Hole *et al.,* 2015). An important feature of the BPIP melting column is that the combination of thick lithosphere (P*f* ~ 2.7 GPa) and T_P ~ 1500°C only allows limited extents of melting and P*m* (~ 2.9 GPa) approaches P*f*. In addition, P*m* = 2.9 GPa requires most magma to have been generated in the garnet-spinel transition of the upper mantle. This combination of P*i*, P*m* and P*f* can only occur for T_P ~ 1500°C and P*f* ~ 2.7 GPa probably requiring a continental setting to achieve. A small increase in T_P or decrease in P*f* or both, would move P*m* into the spinel stability field of the upper mantle as is does for the FIBG. The significance of this will be discussed in the section on REE fractionation below.

Integration of rare earth element data and PRIMELT results.

Many existing studies of the petrogenesis of the igneous rocks of the NAIP have relied on the use of trace elements, and in particular REE profiles, to constrain depths, pressures and therefore, by inference, T_P (e.g. Kerr *et al.,* 1999; Tegner *et al*., 1998; Thompson *et al.,* 1986; 1982; Hole *et al*., 2015). Here, we use the reverse process and examine the trace element characteristics of lavas for which the PRIMELT model provides the conditions of melting. REE data, where they are available, have been fractionation-correct for the amount of olivine accumulation or removal given by the PRIMELT model using the partition coefficients given in Hole *et al*. (2015). Chondrite-normalized rare earth element (REE) profiles are shown in Fig. 10 for selected samples which are light-REE depleted with chondrite normalized La/Sm < 0.1 ($[La/Sm]_N$). These samples also have ΔNb < 0.0 (Fitton *et al.,* 1997) and as such can be considered to have been derived by melting of mantle peridotite similar in composition to that which produces modern MAR MORB distant from the Iceland plume system (Fitton *et al.* 1997; Hole *et al.* 2015). Consequently, we have assumed that the selected samples only differ from one another in the detail of their respective melting regimes. In Fig. 10a-c, samples have been grouped by the lithology of the melting residue as determined from the PRIMELT model. Samples with garnet peridotite residual lithologies exhibit a characteristic convex-upwards shape with $[La/Sm]_N < 1.0$ and $[Tb/Yb]_N > 1.0$, and all have P*m* > 2.9 GPa, a pressure which falls within the range for the spinel-garnet transition of the upper-mantle. The majority of magmas with P*m* < 2.8 with a harzburgite residue have the same REE profiles as primary magmas with a spinel peridotite reside. A small number of samples with a spinel peridotite residue exhibit convex-upwards REE profiles (Fig. 10b) suggesting that the majority of melting to produce these compositions must have taken place in the garnet-spinel transition of the upper mantle, even though the P*f* may be in the spinel stability field of the upper-mantle.

Relationships between $[La/Yb]_N$ and $[Tb/Yb]_N$ have been used by a number of authors (e.g. Hunt *et al.* 2012; Hole *et al.* 2015) to determine 'deep' *versus* 'shallow' melting of peridotite with deeper melting giving progressively higher $[Tb/Yb]_N$ (Fig. 11). The results of the PRIMELT models and observed REE distributions are in general agreement in this respect. Data points for Disko Island samples fall close to a model garnet peridotite melting trajectory and data for Baffin Island basalts plots close to a spinel peridotite melting trajectory (Fig. 11a). However, it is important to note that the precise position of melting trajectories in Fig. 11 is model-dependent. Fig. 11b shows samples for which PRIMELT solutions are available. Samples with a garnet peridotite residue plot in the expected position above the spinel melting trajectory. Samples with a harzburgite residue mainly plot along the spinel melting trajectory, again an expected result. However, samples with a spinel peridotite residue show considerable scatter in Fig. 11b. This is because PRIMELT results give the residue at the final (lowest) pressure of melting. Consequently, primary magmas with P*f* ~ 2.7 may have a spinel peridotite residue, but will exhibit a garnet peridotite REE signature because the majority of melting took place in the garnet stability field of the upper-mantle. This is consistent with P*m* values determined for such samples. We make the observation here that the convex upward REE profiles are only likely to be generated under the specific conditions where P*m* is within the garnet-spinel stability field of the upper-mantle. As we noted above, in the NAIP, this requires the LAB to be at ~ 95 km and T_P ~1500°C which are the prevalent conditions within the BPIP. In Fig. 10d REE patterns are shown for BPIP basalts for which no PRIMELT solution is available, all of which exhibit convex upward REE profiles. For the BPIP as a whole, covariations between $[La/Yb]_N$ and $[Tb/Yb]_N$ (Fig. 11c) are consistent with melting in the garnet-spinel transition of the upper-mantle, with only a small number of basalts having a spinel-only signature. Therefore REE distributions are consistent with T_P =1480 - 1510°C and a depth to the LAB of ~ 90 km.

CONCLUSIONS

Within the NAIP, we have identified sufficient PRIMELT primary magma solutions from a number of locations to provide a framework for T_P variations over a broad geographical area from 61-0 Ma. However, lavas that occupy large sections of the stratigraphy of, for example the BPIP (up to 2 km) and the Beinisvørð Formation and Lopra Formation of the FIBG (> 4 km) do not yield any T_P results. This is because of their evolved nature and their crystallization of an assemblage of olivine + plagioclase ± augite. This leads to relatively large intervals of the NAIP stratigraphy for which methods such as PRIMELT cannot resolve

T_P information. Integration and calibration of alternative approaches such as using REEs to infer relative changes in melting depth (e.g. Tegner *et al.*, 1998) with the PRIMELT method may enable better insight into the time-dependent changes of T_P in the future.

NAIP magmatism can be attributed to a thermal anomaly of ambient T_P (1350°C) +200°C. We can find no evidence of secular cooling of more than ~ 50°C in 61 Ma. The highest T_P of ~ 1550°C is recorded in the Vaigat Formation of West Greenland at ~ 61 Ma although there is some indication of T_P up to 1650°C at this location at 61 Ma. Data for contemporaneous lavas related to the SDRS of East Greenland gives T_P ~ 1456°C suggesting a spatial gradient in T_P. Magmatism in the BPIP required T_P ~ 1500°C at 58-60 Ma, with the possibility that the main plateau-forming lava sequences are slightly lower than this at T_P ~ 1480°C. Latest Palaeocene and earliest Eocene (55-57 Ma) magmatism in East Greenland required T_P ~ 1538°C, whereas contemporaneous lavas within the upper formations of the FIBG required T_P ~ 1519°C. Modern Iceland has a bimodal distribution of T_P, with rift-flank magmatism requiring a lower T_P (~ 1450°C) than rift-zone magmatism (~ 1500°C). For the NAIP as a whole the dominant control on T_P appears to be the proximity to the plume centre, although thermal pulsing of the plume cannot be ruled out based in the current data set, and may be the reason for T_P variations in Iceland at present-day.

Variations in the extent of melting required for the generation of picrites in West Greenland was controlled by the depth to the base of the lithosphere. Melting beneath Disko Island ceased at ~60km deeper that at Baffin Island, the latter having melt column characteristics similar to modern Iceland, but with T_P approximately 50°C hotter. Integration of the results of major element modelling with data for the REE, shows that convex-upwards REE profiles ($[La/Sm]_N < 1.0$ and $[Tb/Yb]_N > 1.0$) can be generated from a LREE-depleted source, at $T_P \geq$ 1480°C where the base of the lithosphere is ≥ 65km in depth. The recognition of such REE profiles is therefore pressure and T_P specific.

651 **ACKNOWLEDGEMENTS**

652 The authors wish to thank Claude Herzberg, Estaban Gazel and an anonymous reviewer
653 for thoughtful and constructive reviews.

654

References cited.

Adria, P., Hirschmann, M.M., Withers, A.C. & Tenner, T.J. (2012). H_2O storage capacity of olivine at 5–8GPa and consequences for dehydration partial melting of the upper mantle. *Earth and Planetary Science Letters*, **345-358**, 104-116.

Albarède, F. (1992). How deep do common basaltic magmas form and differentiate? *Journal of Geophysical Research*, **97**, 10997–11009.

Archer, S.A., Bergman, S.C., Illiffe, J., Murphy, C.M. & Thorton, M. (2005). Palaeogene igneous rocks reveal new insights into the geodynamic evolution and petroleum potential of the Rockall Trough, NE Atlantic Margin. *Basin Research*, **17**, 171-201.

Baker, M.B. & Beckett, J.R. (1999). The origin of abyssal peridotites: a reinterpretation of constraints based on primary bulk compositions. *Earth and Planetary Science Letters*, **171**, 49-61.

Barnhoorn, A., van der Wal, W. & Drury, M.R. (2011). Upper mantle viscosity and lithospheric thickness under Iceland. *Journal of Geodynamics*, **52**, 260-270.

Barrat, J.A. & Nesbitt, R.W. 1996. Geochemistry of Tertiary volcnaism of Northern Ireland. *Chemical Geology*, **129**, 15-38.

Chambers, L.M. & Pringle, M.S. (2001). Age and duration of activity at the Isle of Mull Tertiary igneous centre, Scotland, and confirmation of the existence of subchrons during Anomaly 26r. *Earth and Planetary Science Letters,* **193**, 333-345.

Coogan, L.A., Saunders, A.D. & Wilson, R.N. (2014). Aluminium-in-olivine thermometry of primitive basalts: Evidence of an anomalously hot mantle source for large igneous provinces. *Chemical Geology*, **368**, 1-10.

Courtier, A.M. (2007). Correlation of seismic and petrological thermometers suggests deep thermal anomalies beneath hotspots, Earth and Planetary Science Letters, **264**, 308–316.

Cramer, E.L., Sherlock, S.C., Halton, A.M., Blake, S., Barry, T.L., Kelley, S.P. & Jolley, D.W. (2013). Which age is the true age? Unravelling within-flow $^{40}Ar/^{39}Ar$ age variations in Faroe Islands basalt lavas. *Goldschmidt Conference Abstract*, Florence, Italy.

Dale, C.W., Pearson, D.G., Starkey, N.A., Stuart, F.M., Ellam, R.M., Larsen, L.M., Fitton J.G & Macpherson, C.G. (2009). Osmium isotopes in Baffin Island and West Greenland picrites: Implications for the $^{187}Os/^{188}Os$ composition of the convecting mantle and the nature of high $^3He/^4He$ mantle. *Earth and Planetary Science Letters*, **278**, 267-277.

Dasgupta, R., Hirschmann, M.M. & Smith, N.D. (2007). Partial melting experiments on peridotite + CO_2 at 3 GPa and genesis of alkalic ocean island basalts, *Journal of Petrology*, **48**, 2093-2124.

Dickin, A.P., Jones, N.W., Thirlwall, M.F. & Thompson, R.N. (1987). A Ce/Nd isotope study of crustal contamination processes affecting Paleocene magmas in Skye, Northwest Scotland. *Contributions to Mineralogy & Petrology,* **96**, 455-464.

Ebdon, C.C., Granger, P.J., Johnson, H.D. & Evans, A.M. (1995). Early Tertiary evolution and sequence stratigraphy of the Faeroe-Shetland Basin: implications for hydrocarbon prospectivity. In: Scrutton, R. A., Stoker, M. S., Shimmield, G. B. & Tudhope, A. W. (eds), 1995, *The Tectonics, Sedimentation and Palaeoceanography of the North Atlantic Region*, Geological Society Special Publications, **90**, 51-69.

Fitton, J.G., Saunders, A.D., Norry, M.J., Hardarson, B.S. & Taylor R.N. (1997). Thermal and chemical structure of the Iceland plume. *Earth and Planetary Science Letters*, **153**, 197-208.

Foulger, G.R. (2012). Are 'hot spots' hot spots ? *Journal of Geodynamics*, **58**, 1-28.

Fowler, S.J., Bohrson, W.A. & Spera, F.J. (2003). Magmatic Evolution of the Skye Igneous Centre, Western Scotland: Modelling of Assimilation, Recharge and Fractional Crystallization. *Journal of Petrology*, **45**, 2481-2505.

Ganerød, M., Smethurst, M.A., Torsvik, T.H., Prestvik, T., Rousse, S., McKenna, C., van Hinsbergen, D.J.J. & Hendriks B.W.H. (2010). The North Atlantic Igneous Province reconstructed and its relation to the Plume Generation Zone: the Antrim Lava Group revisited. *Geophysical Journal International*, 182, 183-202.

Gazel, E., Hoernle, K., Carr, M.J., Herzberg, C, Saginor, I., van den Bogaard, P., Hauff, F., Feigenson, M., & Swisher III, C., (2011). Plume–subduction interaction in southern Central America: Mantle upwelling and slab melting. *Lithos*, **121**, 117-134.

Gill, R.C.O., Pedersen, A.K. & Larsen, J.G. (1992). Tertiary picrites in West Greenland: Melting at the periphery of a plume? *In:* Storey, B. C., Alabaster, T. & Pankhurst, R. J. (eds) *Magmatism and the causes of Continental Break-Up* Geological Society, London, Special Publications, **68,** 335-348.

Hamilton, M.A., Pearson, D.G., Thompson, R.N., Kelley, S.P. & Emeleus, C.H. (1998). Rapid eruption of Skye lavas inferred from precise U–Pb and Ar–Ar dating of the Rum and Cuillin plutonic complexes. *Nature*, **384**, 260-263.

Hards,V. L., Kempton, P. D., Thompson, R. N. & Greenwood, P. B. (2000). The magmatic evolution of the Snaefell volcanic centre: an example of volcanism during incipient rifting in Iceland. *Journal of Volcanology and Geothermal Research* **99**, 97-121.

Hardarson, B.S., Fitton, J.G, Ellam, R.M. & Pringle, M.S., (1997). Rift relocation - a geochemical and geochronological investigation of a palaeo-rift in northwest Iceland, *Earth and Planetary Science Letters*, **153**, 181-196.

Herzberg, C. (2004a). Partial Crystallization of Mid-Ocean Ridge Basalts in the Crust and Mantle. *Journal of Petrology*, **45**, 2389-2405.

Herzberg, C. (2004b). Geodynamic information in peridotite petrology. *Journal of Petrology* **45**, 2507–2530.

Herzberg, C. (2006). Petrology and thermal structure of the Hawaiian plume from Mauna Kea volcano. *Nature***, 444,** 605-609.

Herzberg, C. & O'Hara, M.J. (2002). Plume-associated ultramafic magmas of Phanerozoic age, *Journal of Petrology*, **43**, 1857-1883.

Herzberg, C. & Asimow, P.D. (2008). Petrology of some oceanic island basalts: PRIMELT2.XLS software for primary magma calculation. *Geochemistry, Geophysics, Geosystems*, **9**.

Herzberg, C. & Gazel, E. (2009). Petrological evidence for secular cooling in mantle plumes. *Nature*, **458**, 619-623.

Herzberg, C. & Asimow, P.D. (2015). PRIMELT3 MEGA.XLSM software for primary magma calculation: Peridotite primary magma MgO contents from the liquidus to the solidus. *Geochemistry, Geophysics, Geosystems*, 16, 563-578.

Herzberg, C., Asimow, P.D., Arndt, N., Niu, Y., Lesher, C.M., Fitton, J.G., Cheadle, M.J. & Saunders, A.D. (2007). Temperatures in ambient mantle and plumes: Constraints from basalts, picrites, and komatiites. *Geochemistry, Geophysics, Geosystems,* **8**, 1-34.

Hole, M.J. & Saunders, A.D. (1996). The generation of small melt-fractions in truncated melt columns: Constraints from magmas erupted above slab windows and implications for MORB genesis. *Mineralogical Magazine*, **60**, 173-189.

Hole, M.J. (2015). The generation of continental flood basalts by decompression melting of internally heated mantle. *Geology*, **43**, 311-314.

Hole. M.J., Millett, J.M., Rogers, N.W. & Jolley, D.W. (2015). Rifting and mafic magmatism in the Hebridean basins. *Journal of the Geological Society*, London, **172**, 218-236.

Howell, S.M., Garrett, I., Breivik, A.J., Rai, A., Mjelde, R., Hanan, B., Sayit, K. & Vogt, P. (2014). The origin of the asymmetry in the Iceland hotspot along the Mid-Atlantic Ridge from continental break-up to present day. *Earth and Planetary Science Letters*, **392**, 143-153.

Hunt, A.C., Parkinson, I.J., Harris, N.B.W., Barry, T.L., Rogers, N.W. & Yondon, M. (2012). Cenozoic volcanism on the Hangai Dome,central Mongolia: geochemical evidence for changing melt sources and implications for mechanisms of melting. *Journal of Petrology*, **53**, 1913-1942.

Jamtveit, B., Brooker, R., Brooks, K., Larsen, L.M. & Pedersen, T. (2001). The water content of olivines frojm the North Atlantic Volcanic Province. *Earth and Planetary Science Letters*, **186**, 401-415.

Jolley, D.W. & Bell, B.R. (1997). Application of palynological data to the chronology of the Palaeogene lava fields of the British Province: Implications for magmatic stratigraphy. *Journal of the Geological Society, London*, **154**, 701-708.

Kent, R.W. & Fitton, J.G. (2000). Mantle sources and melting dynamics in the British Palaeogene Igneous Province. *Journal of Petrology*, **41**, 1023-1040.

Kerr, A.C., Kent, R.W., Thomson, B.A., Seedhouse, J.K. & Donaldson, C.H. (1999). Geochemical Evolution of the Tertiary Mull Volcano, Western Scotland. *Journal of Petrology,* **40**, 873-908.

Klein, E.M. & Langmuir, C.H. 1987. Global correlations of ocean ridge basalt chemistry with axial depth and crustal thickness. *Journal of Geophysical Research*, **92**, 8089-8115.

Larsen L. M. & Pedersen A. K. (2000). Processes in high-Mg, high-T magmas: evidence from olivine, chromite and glass in Paleogene picrites from West Greenland. *Journal of Petrology*, **41**, 1071-1098

Larsen, L.M. & Pedersen, A.K. (2009). Petrology of the Paleocene Picrites and Flood Basalts on Disko and Nuussuaq,West Greenland. *Journal of Petrology*, **50**, 1667-1711.

Larsen, L.M., Waagstein, R., Pedersen, A. K. & Storey, M. (1999). Trans-Atlantic correlation of the Palaeogene volcanic successions in the Faeroe Islands and East Greenland. *Journal of the Geological Society*, **156**, 1081–1095.

Larsen, L.M., Heaman, L.M., Creaser, R.A., Duncan, R.A., Frei, R. & Hutchison, M. (2009) Tectonomagmatic events during stretching and basin formation in the Labrador Sea and the Davis Strait: evidence from age and composition of Mesozoic to Palaeogene dyke swarms in West Greenland. Journal of the Geological Society, London, 166, 999-1012.

Larsen, L.M., Oedersen, A.K., Tegner, C. & Duncan R.A. (2014). Eocene to Miocene igneous activity in NE Greenland: northward younging of magmatism along the East Greenland margin. *Journal of the Geological Society, London*, **171**, 539-553.

Larsen L.M., Pedersen, A.K., Tegners, C., Duncan, R.A., Hald, N. & Larsen, J.G. (2015). Age of Tertiary volcanic rocks on the West Greenland continental margin: volcanic evolution and event correlation to other parts of the North Atlantic Igneous Province. *Geological Magazine*. doi:10.1017/S0016756815000515

Lawver, L.A. & Müller, R.D. (1994). The Iceland hotspot track. *Geology*, **22**, 311–314.

Lee, C-T. A., Lenardic, A., Cooper, C.M., Niu, F. & Levander, A. (2005). The role of chemical boundary layers in regulating the thickness of continental and oceanic thermal boundary layers. *Earth and Planetary Science Letters*, **230,** 379-395.

Lee, C-T. A., Luffi, P., Plank, T., Dalton, H. & Leeman, W.P. (2009). Constraints on the depths and temperatures of basaltic magma generation on Earth and other terrestrial planets using new thermobarometers for mafic magmas. *Earth and Planetary Science Letters*, **279**, 20-33.

Lightfoot, P.C., Hawkesworth, C.J., Olshefsky, K., Green, T. Doherty, W & Keays, R.R. 1997. Geochemistry of Tertiary tholeiites and picrites from Qeqertarssuaq (Disko Island) and Nuussuaq, West Greenland with implications for the mineral potential of comagmatic intrusions. *Contributions to Mineralogy and Petrology*, **128**, 139-163.

Maclennan, J., McKenzie, D. & Gronvøld, K. (2001). Plume-driven upwelling under central Iceland. *Earth and Planetary Science Letters,* **194**, 67-82.

Mattsson, H. B. & Oskarsson, N. (2005). Petrogenesis of alkaline basalts at the tip of a propagating rift: evidence from the Heimey volcanic center, south Iceland. Journal of *Volcanology and Geothermal Research*, **147,** 245-267.

Mihalffy, P., Steinberger, B. & Schmeling, H. 2008.The effect of the large-scale mantle flow field on the Iceland hotspot track. *Tectonophysics*, **447**, 5–18

Millett, J.M., Hole, M.J., Jolley, D.W., Schofield, N. & Campbell, E. 2015. Frontier exploration and the North Atlantic Igneous Province: new insights from a 2.6 km offshore volcanic sequence in the NE Faroe-Shetland Basin. *Journal of the Geological Society, London*. doi:10.1144/jgs2015-069.

Murton, B.J., Taylor, R.N. & Thirlwall, M.F. (2002). Plume-ridge interaction: a geochemical perspective from the Reykjanes Ridge. *Journal of Petrology*, **43**, 1155-1176.

Nichols, A.R.L., Carroll, M.R. & Hoskulsson, A. (2002). Is the Iceland hot spot also wet? Evidence from the water contents of undegassed submarine and subglacial pillow basalts. *Earth and Planetary Science Letters*, **202**, 77-87.

Nielsen, S.B., Stephenson, R.A. & Thomsen, E. (2007). Dynamics of Mid-Palaeocene North Atlantic rifting linked with European intra-plate deformations. *Nature*, **450**, 1071-1074

Parnell-Turner, R.E., White, N.J., Maclennan, J, Henstock, T.J., Murton, B.J. & Jones, S.M. (2013). Crustal manifestations of a hot transient pulse at 60°N beneath the Mid-Atlantic Ridge. *Earth and Planetary Science Letters*, **363**, 109-120.

Parnell-Turner, R., White, N., Henstock, T, Murton, B., Maclennan, J., & Jones, S.M., (2014). A continuous 55-million-year record of transient mantle plume activity beneath Iceland. *Nature Geoscience*, **7**, 914-919.

Passey, S.R. & Jolley, D.W. (2009). A revised lithostratigraphic nomenclature for the Palaeogene Faroe Islands Basalt Group, NE Atlantic Ocean. *Earth and Environmental Science Transactions of the Royal Society of Edinburgh*, **99**, 127-158.

Pearson, D.G., Emeleus, C.H. & Kelley, S.P. (1996). Precise $^{40}Ar/^{39}Ar$ age for the initiation of Palaeogene volcanism in the Inner Hebrides and its regional significance. *Journal of the Geological Society*, *London*, **158**, 815-818.

Peate, D.W., Barker, A.K., Riishuus, M.S. & Andreasen, R. (2008). Temporal variations in crustal assimilation of magma suites in the East Greenland flood basalt province: Tracking the evolution of magmatic plumbing systems. *Lithos*, **102**, 179-197.

Peate, D.W., Breddam, K., Baker, J.A., Kurz, M.D., Barker, A.K., Prestvik, T., Grassinaeu, N., & Skogvaard, C. (2010). Compositional characteristics and spatial distribution of enriched Icelandic mantle components. *Journal of Petrology*, **51**, 1447-1475.

Peate, D.W., Peat, I.U., Rowe, M.C., Thompson, J.M. & Kerr, A.C. (2012). Petrogenesis of High-MgO lavas of the Lower Mull Plateau Lava Formation, Scotland: insights from melt inclusions. *Journal of Petrology,* **53**, 1867-1886

Peslier, A.A. & Bizimis, M. (2015). Water in Hawaiian peridotite: A case study for a dry metasomatized oceanic mantle lithosphere. *Geochemistry, Geophysics, Geosystems,* **16**, 1211-1232.

Poore, H.R., White, N. & Jones, S. 2009. A Neogene chronology of Iceland plume activity from V-shaped ridges. *Earth and Planetary Science Letters*, **283**, 1-13.

Putirka, K.D. (2008). Thermometers and Barometers for Volcanic Systems. *Reviews in Mineralogy & Petrology*, **69**, 61-120.

Putirka, K.D., Perfit, M., Ryerson, F.J. & Jackson, M.G. (2007). Ambient and excess mantle temperatures, olivine thermometry, and active vs. passive upwelling. *Chemical Geology*, **241**, 177-206.

Robinson, J.A.C. & Wood, B.J. (1998). The depth of the spinel to garnet transition at the peridotite solidus. *Earth and Planetary Science Letters*, 164, 277-284.

Saunders, A.D., Fitton J.G., Kerr, A.C., Norry, M.J. & Kent, R.W. (1997). The North Atlantic Igneous Province. In: Mahoney, J.J. & Coffin, M.F. (eds) *Large Igneous Provinces: Continental, Oceanic and Planetary Volcanism*. Geophysical Monograph, American Geophysical Union, 100, 45-93.

Scarrow, J.H. & Cox, K.G. (1995). Basalts generated by decompressive adiabatic melting of a mantle plume: a case study from the Isle of Skye, NW Scotland. *Journal of Petrology*, **36**, 3-22.

Scarrow, J.H., Curran, J.M. & Kerr, A.C. (2000). Major element records of variable plume involvement in the North Atlantic Province Tertiary Flood Basalts. *Journal of Petrology* **41**, 1155-1176.

Shorttle, O., Maclennan, J. & Lambart, S. (2014). Quantifying lithological variability in the mantle. *Earth & Planetary Science Letters*, **395**, 24-40.

Starkey, A.A., Stuart, F.M., Ellam, R.M., Fitton J.G., S, Basu & Larsen L. M. 2009. Helium isotopes in early Iceland plume picrites: constraints on the composition of high $^{3}He/^{4}He$ mantle. *Earth and Planetary Science Letters*, **277**, 91-100.

Sun, S-S. & McDonough, W.F. (1988). Chemical and isotopic systematics of oceanic basalts: implications for mantle composition and processes. In: Saunders, A. D. & Norry, M. J. (eds) *Magmatism in the ocean basins*. Geological Society, London, Special Publications, **42,** 313-345.

Tegner, C., Lesher, C.E., Larsen, L.M. & Watt, W.S. (1998). Evidence from the rare-earth-element record of mantle melting for cooling of the Tertiary Iceland plume. *Nature*, **395**, 591–594.

Thompson, R.N. & Morrison, M.A. (1988). Asthenospheric and lower lithospheric mantle contributions to continental extensional magmatism: an example from the British Tertiary Province. *Chemical Geology,* **68,** 1-15.

Thompson, R.N., Dickin, A.P., Gibson, I.L. & Morrison, M.A. (1982). Elemental fingerprints of isotopic contamination of Hebridean Palaeocene mantle-derived magmas by Archaean Sial. *Contributions to Mineralogy and Petrology,* **79**, 159-168.

Thompson, R.N., Morrison, M.A., Dickin, A.P., Gibson, I.L. & Harmon, R.S. (1986). Two contrasting styles of interaction between basic magmas and continental crust in the British Tertiary Volcanic Province. *Journal of Geophysical Research* , **91,** 5985-5997.

Trela, J., Vidito, C., Gazel, E., Herzberg, C., Class, C., Whalen, W., Jicha, B., Bizimis, M. & Alvarado, G.E. (2015). Recycled crust in the Galpagos plume source at 70 Ma; implications for plume evolution. *Earth and Planetary Science Letters*, **425**, 268-277.

887 Waight, T.E. & Baker, J.A. (2012). Depleted basaltic lavas from the Proto-Iceland plume, central East Greenland. *Journal of Petrology*, **53**, 1569-1596.

889 Walter, M. J. 1998. Melting of garnet peridotite and the origin of komatiite and depleted lithosphere, *Journal of Petrology*, **39**, 29-60.

891 Yaxley, G.M., Kamanetsky, V.S., Kamanestsky, M., Norman, M.D. & Francis, D. (2004). Origins of compositional heterogeneity in olivine-hosted melt inclusions from the Baffin Island picrites. Contributions to Mineralogy ans Petrology, 148, 426-442.

Figure Captions.

Fig. 1 a) (a) Map of the continental shelf west of the British Isles showing the position of onshore and offshore igneous centres and dyke swarms. Pecked lines labelled "Lawver & Muller" and "Mihalffy *et al*." are the extents of the plume influence according to Lawver & Müller (1994) and Mihalffy *et al.* (2008). After Hole *et al.* (2015). b) reconstruction of the North Atlantic region at about 65 Ma giving the locations of places referred to in the text.

Fig. 2. Stratigraphy of the BPIP and adjacent areas from 65-50 Ma, modified and updated after Jolley & Bell (2002). Depositional sequences labelled T10 to T60 are from Ebdon *et al.* (1995). Absolute ages; Skye and Rum intrusions, Hamilton *et al.* (1998); 164/170-1 sills, Archer *et al.* (2005); Antrim basalts, Ganerod *et al.* (2009); Eigg lavas, Pearson *et al.* (1996); Greenland, Larsen *et al.* (2009; 2014; 2015).

Fig. 3 a) Schematic pressure-temperature diagram illustrating the petrogenesis of an olivine-phyric basalt (BI/CS/8; Dale *et al.,* 2009) with 9.7 wt% MgO which fractionated 28% olivine and erupted with a liquidus temperature of ~ 1420°C. The primary magma to this basalt is calculated to contain 19.0 wt% MgO, requiring T_P ~ 1540°C. P*i* = 4.2 GPa, and is calculated from the intersection of the dry peridotite solidus and the 1540°C adiabat. The primary magma ascended along the olivine liquidus as indicated by the arrows, which also corresponds to the 19.0 wt% MgO isopleth. The extent of melting, *FAFM* ~ 0.30, is calculated from phase equilibria. The final pressure of melting, P*f*, is estimated to be 1.9 GPa for this sample. The mean pressure of melting P*m* = 2.6 GPa at 1550°C. Note that initial melting takes place in equilibrium with garnet peridotite, but the majority of melting takes place in the spinel stability field of the upper-mantle. P*i* was calculated according to the schemes of Herzberg & Gazel (2009) and Gazel *et al.* (2011) and P*m* was calculated using the method of Lee *et al.* (2009). Details of P*f* calculations are given in Electronic Appendix 2. The dry peridotite solidus is taken from Herzberg & Asimow (2015) and numbers in italics represent MgO content of primary magmas formed along the solidus, which are the starting points for the MgO isopleths. 'Garnet in' and 'spinel out' boundaries are from Robinson & Wood (1998).

Fig. 4. a) FeO *versus* MgO for modelled primary magma compositions showing initial pressure of melting (P*i*; pecked lines with arrows) final pressure of melting (P*f*; solid lines) and melt fraction (*F-AFM*; thin pecked lines) for melting of mantle peridotite KR-4003. Note that Baffin Island primary magmas mostly have P*f* < 2.0 whereas Disko Island have P*f* ~ 2.0

to > 3.0 GPa. Baffin Island primary magmas occupy a similar position in this diagram to those for the Ontong-Java Plateau. Primary magma compositions are from this study, Herzberg & Gazel (2009) and Hole (2015). b) molecular projection of primary magma compositions onto the plane olivine-anorthite-quartz (Ol-An-Qz) from or towards diopside ([Di]) showing the stability fields for garnet peridotite, spinel peridotite and harzburgite in relationship to extent of melting (*FAFM*). Note that Baffin Island primary magmas mostly separated from a harzburgite residue, whereas Disko Island primary magmas mostly separated from a garnet peridotite residue, requiring Baffin Island basalts to have lower P*f* than Disko Island. Sample BI/CS/8 which is shown in Fig. 3, is indicated in both a) and b) and its calculated primary magma composition is consistent with final separation from a harzburgite residue. Both a) and b) are after Herzberg & Asimow (2008; 2015). Further details of these figures are given in Electronic Appendix 2 and 3.

Fig. 5. Final pressure of melting (P*f*) *versus* temperature (T°C) for NAIP basalts which yield PRIMELT solutions for melting of dry mantle peridotite. Dotted lines are olivine liquidi with the potential temperature indicated. Pecked lines are contours of constant MgO in the primary magma with wt% MgO indicated by crosses on the peridotite solidus. a) Vaigat Formation picrites and basalts from Disko Island and Baffin Island; b) British Palaeocene tholeiites and basalts along with Faroe Islands Basalt Group. Filled diamonds are PRIMELT solutions derived from melt inclusions trapped in olivine phenocrysts in MPLF lavas; c) Iceland rift zones and rift flanks. Data and sources are given in the electronic Appendix 4.

Fig. 6. Histograms showing T_P distributions for basalts of the NAIP. 1548±32°C is the mean T_P and 2σ for Disko Island.

Fig.7. Histograms of accumulated melt-fraction produced (*F-AFM*) for NAIP primary magmas.

Fig. 8. Histograms of mean pressure of melting (P*m*) for NAIP magmas. The cross-hatched area represents the garnet-spinel transition in the upper mantle. The range of P*m* for Siqueiros MORB is shown in the bottom frames for reference. P*m* was calculated using the scheme of Lee *et al*. (2009).

Fig. 9. Diagrammatical representations of melting columns for various locations in the NAIP, MORB from the Siqueiros Fracture Zone, and basalts from the Ontong-Java Plateau. P*i*, P*f* and P*m* are melting column-averaged data for the location named. The garnet-in boundary and garnet-spinel transition are taken from Robinson & Wood (1998) and are those used by

PRIMELT3. Melting with harzburgite as the residue is not directly correlated with pressure of melting but with extent of melting and so the harzburgite fields are schematic. Note that Siqueiros MORB, Iceland rift-flanks, BPIP and Faroe-Shetland Basin melting columns have P*f* ≈ P*m*.

Fig. 10. Chondrite-normalized (Sun & McDonough, 1988) REE abundances for NAIP basalts with $[La/Sm]_N < 1.0$ and $\Delta Nb < 0$. a) samples with a garnet peridotite residue; b) samples with a spinel peridotite residue and P*f* = 2.8-3.1 GPa; c) samples with a harzburgite residue and P*f* < 2.8 GPa; d) samples from the BPIP with convex-upwards REE profiles consistent with melting in the garnet-spinel transition of the upper mantle but for which no PRIMELT solutions are available. Figures parentheses after the sample names are T_P and *F* respectively. The pecked field on each diagram is the range of REE abundances for melting leaving a harzburgite residue at P*m* < 2.8 GPa. Data sources for BPIP samples; Antrim Plateau, Barrat & Nesbitt (1996); MPLF, Kerr *et al*. (1999); CMT, Hole *et al*. (2015) and Kent & Fitton (2000).

Fig. 11. Plot of $[Tb/Yb]_N$ *versus* $[La/Yb]_N$ for a) all Baffin Island and Disko Island depleted ($\Delta Nb < 0$) basalts. Data sources; Baffin Island, Dale *et al*. (2009); Disko Island, Lightfoot *et al.* (1997) and Larsen & Pedersen (2000). b) NAIP depleted basalts for which PRIMELT solutions are available, indexed by the mineralogy of the residue with which they were in equilibrium at the time of extraction. c) NAIP samples for which no PRIMELT solutions are available. In all diagrams, continuous lines with crosses are melting trajectories garnet and spinel peridotite for a starting composition the same as that for 'non-plume' MAR MORB basalts (Hole *et al.* 2015; Murton *et al.* 2002) with crosses are at 1% melt intervals. After Hunt *et al.* (2012). Horizontal contours for *F* are schematic only. As a first approximation, our PRIMELT database shows that for T_P=1500-1550°C melting occurs at a melt column-averaged rate of ~13% GPa^{-1}.

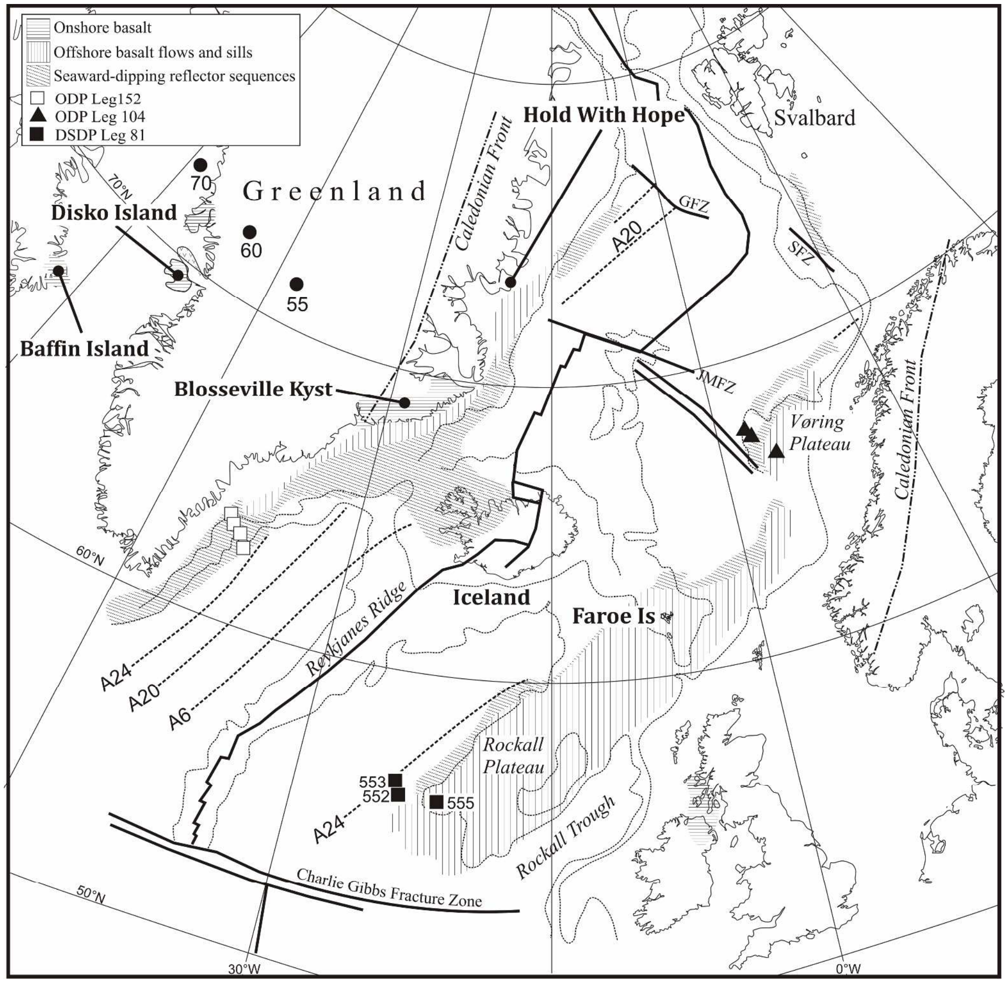

268x261mm (300 x 300 DPI)

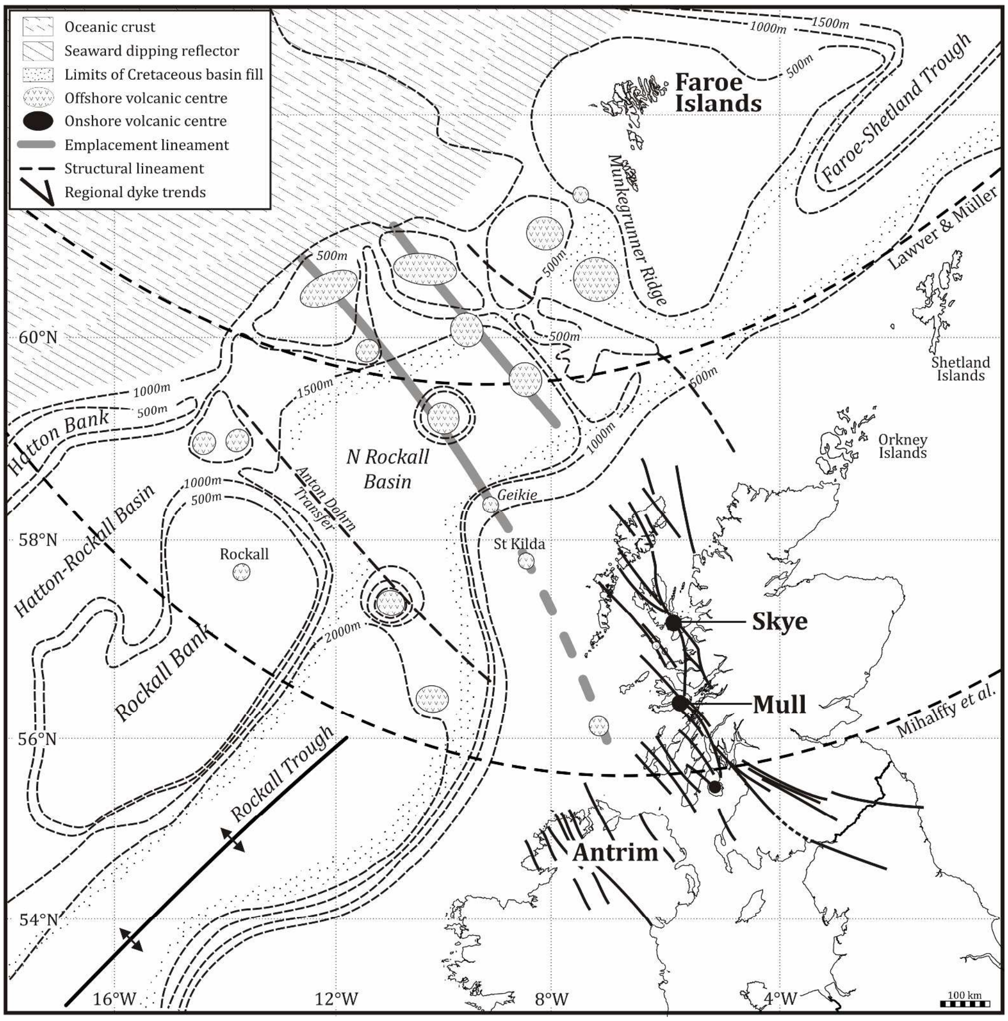

267x270mm (300 x 300 DPI)

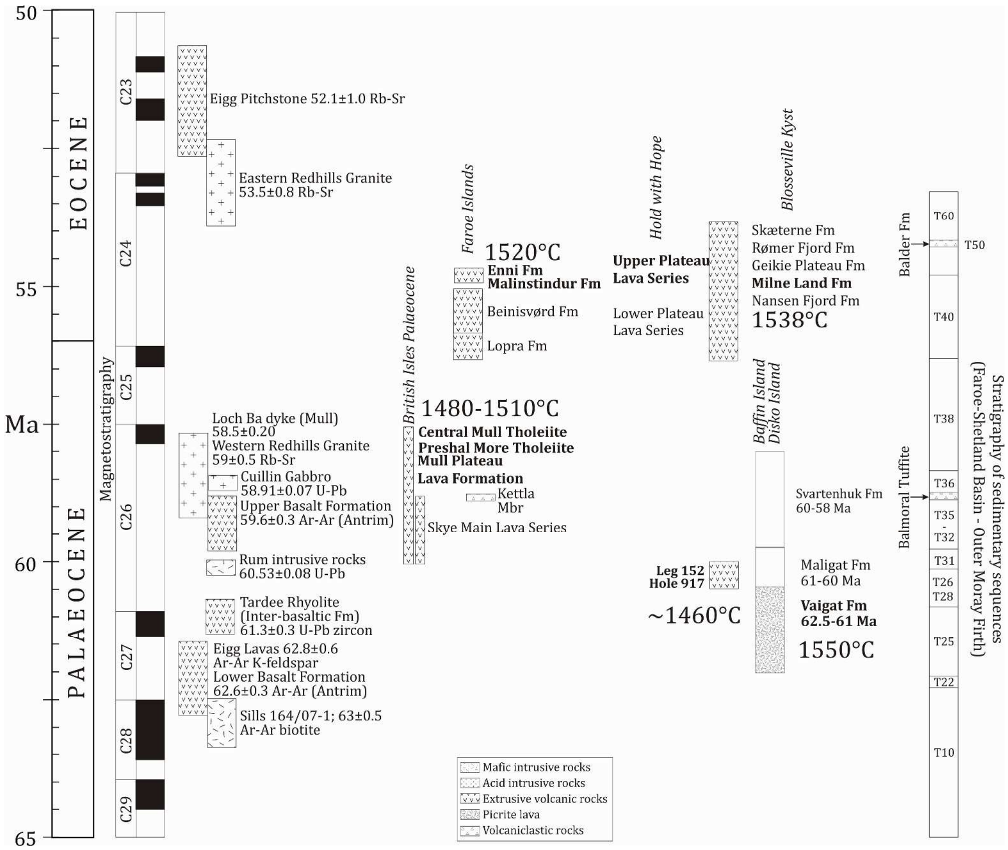

521x437mm (300 x 300 DPI)

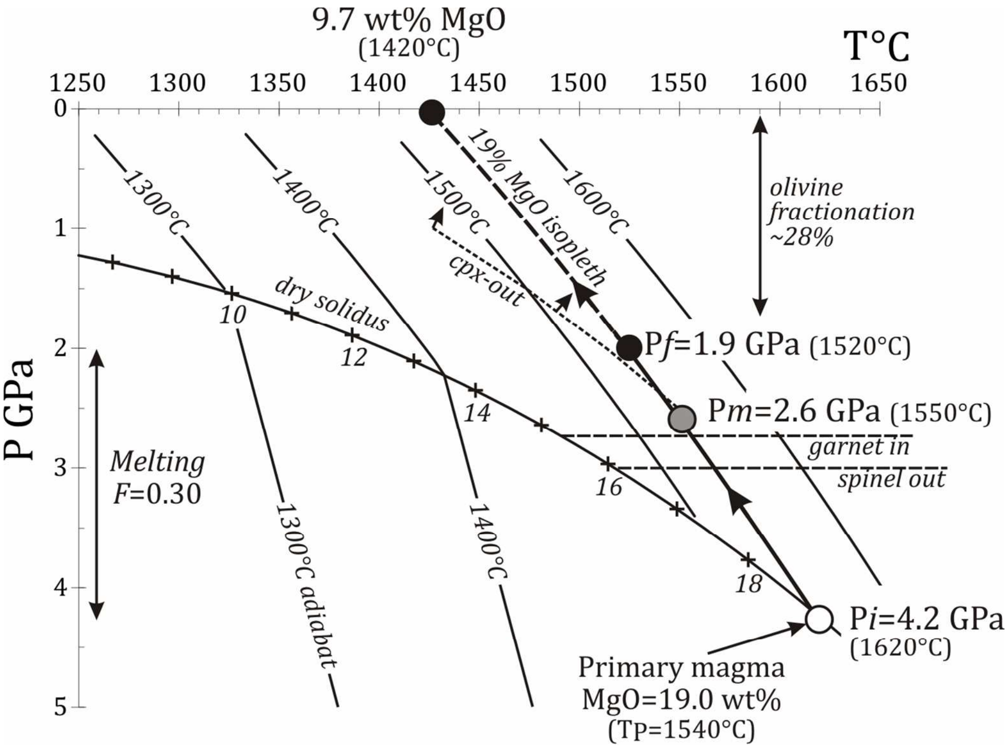

185x136mm (200 x 200 DPI)

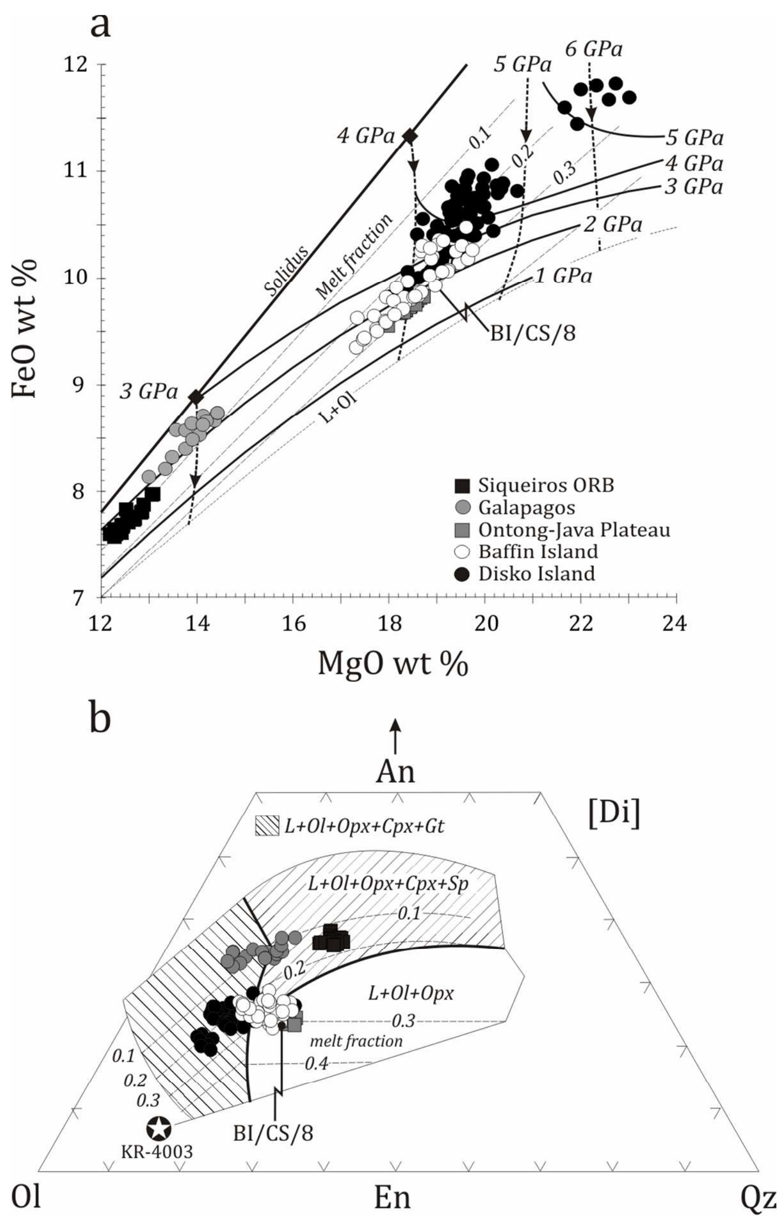

140x219mm (200 x 200 DPI)

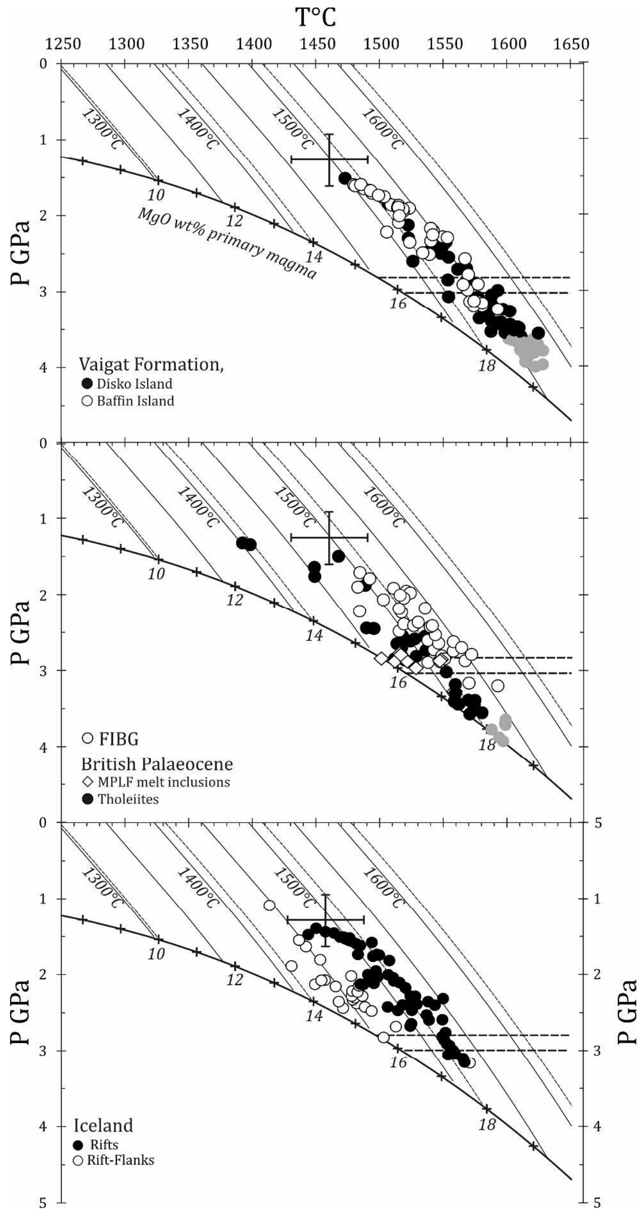

183x350mm (300 x 300 DPI)

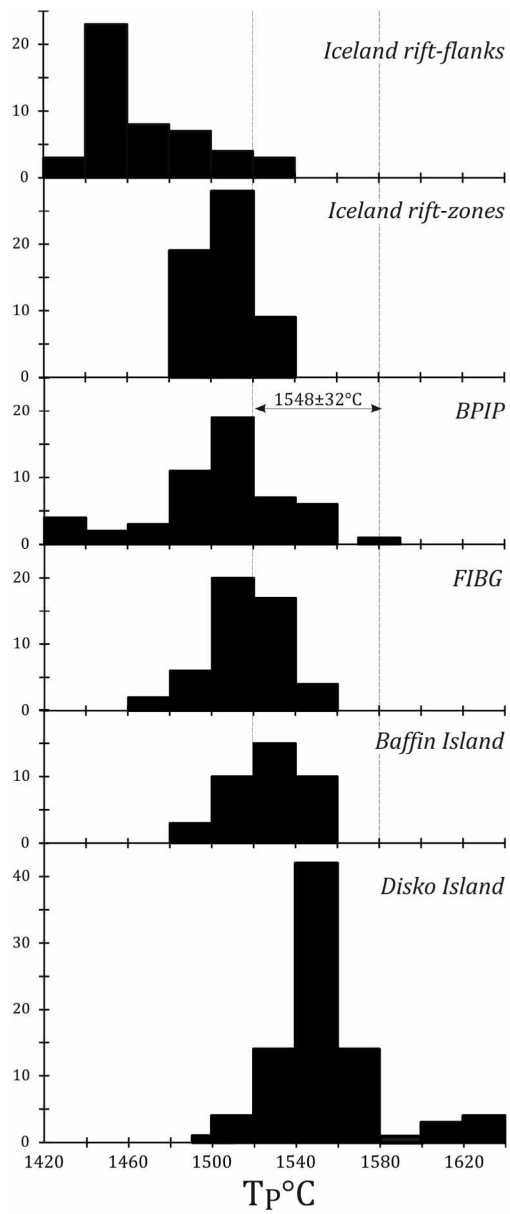

113x276mm (200 x 200 DPI)

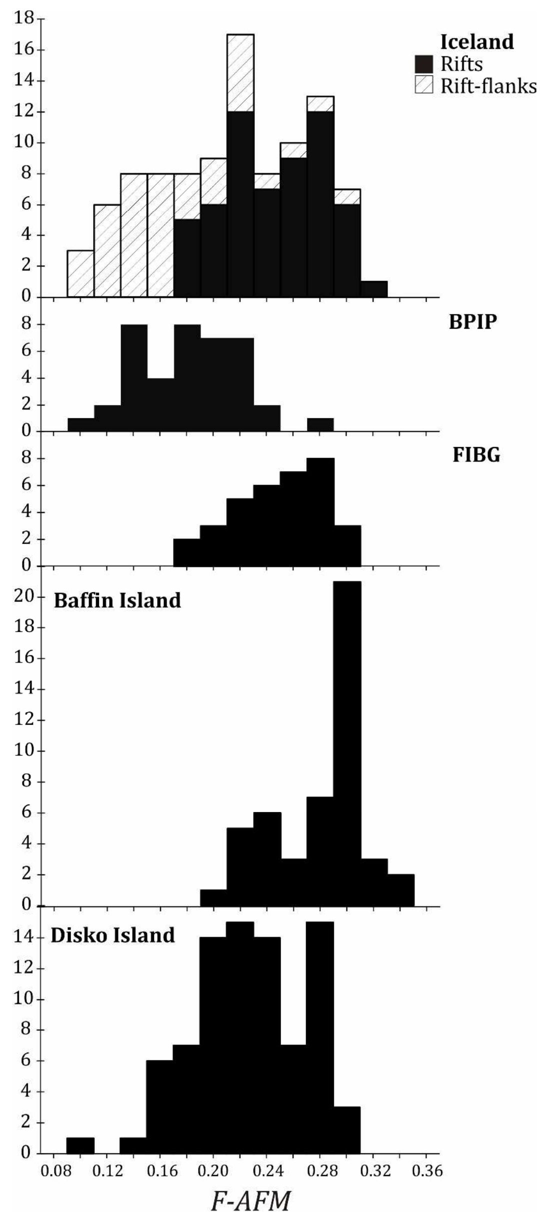

151x346mm (300 x 300 DPI)

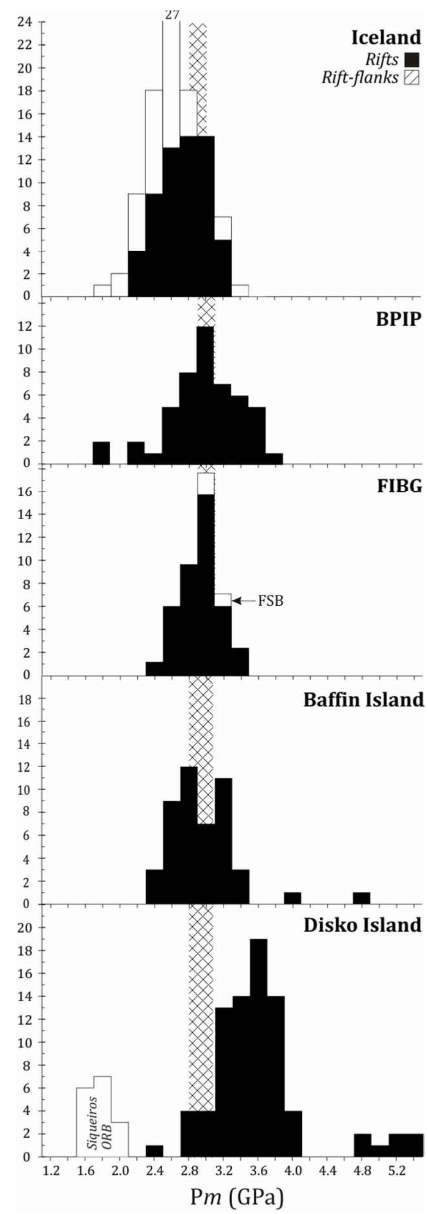

72x212mm (200 x 200 DPI)

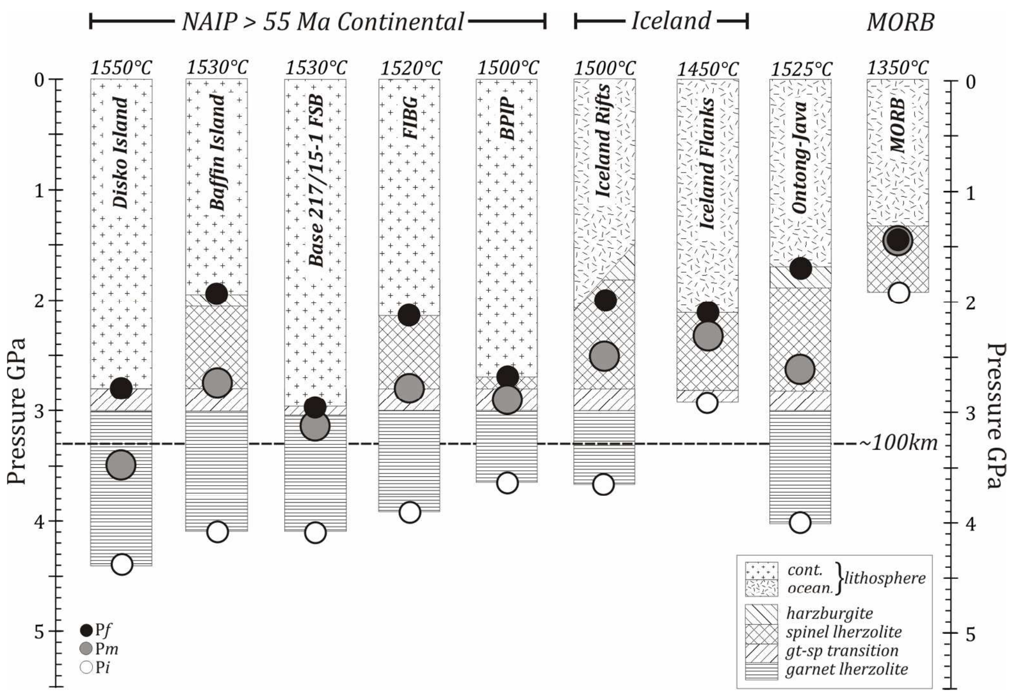

240x163mm (200 x 200 DPI)

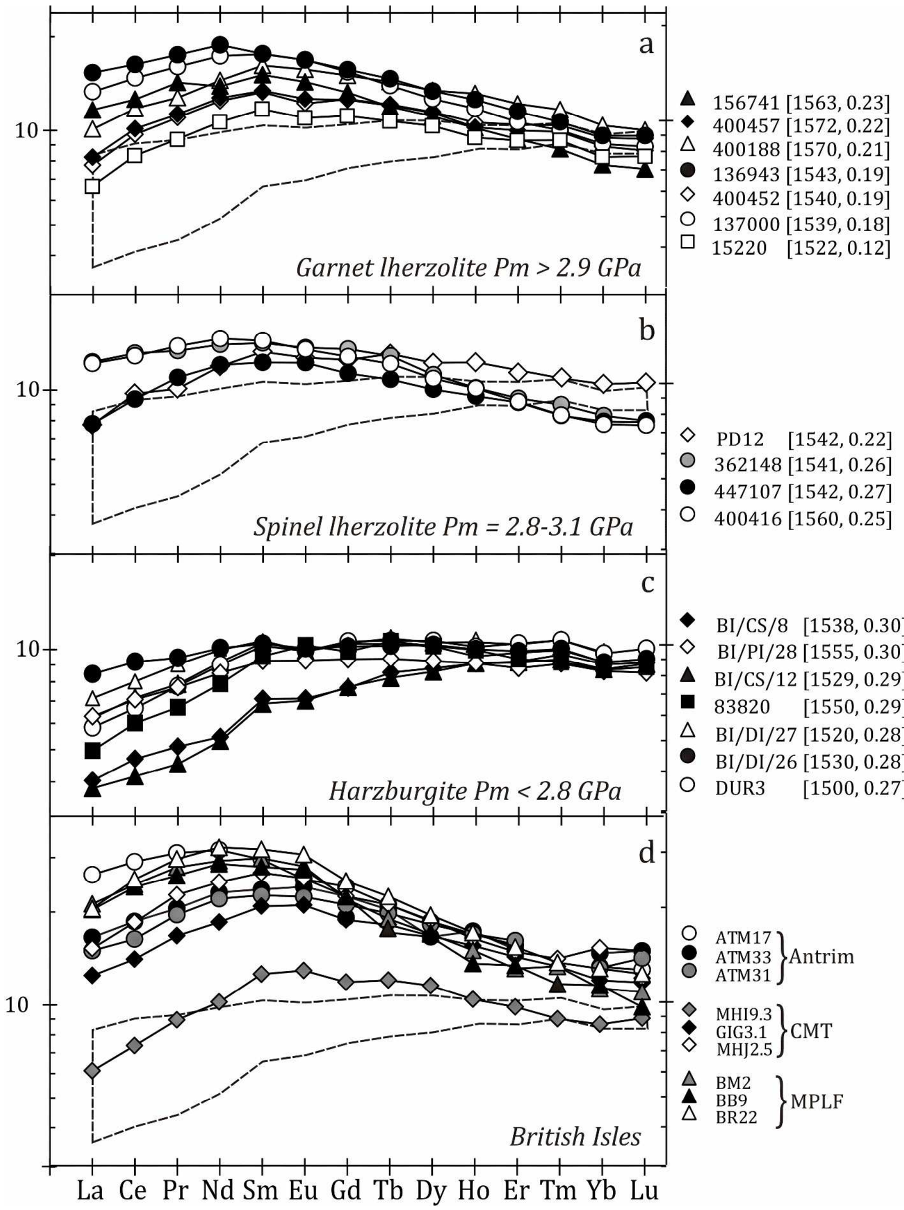

233x309mm (300 x 300 DPI)

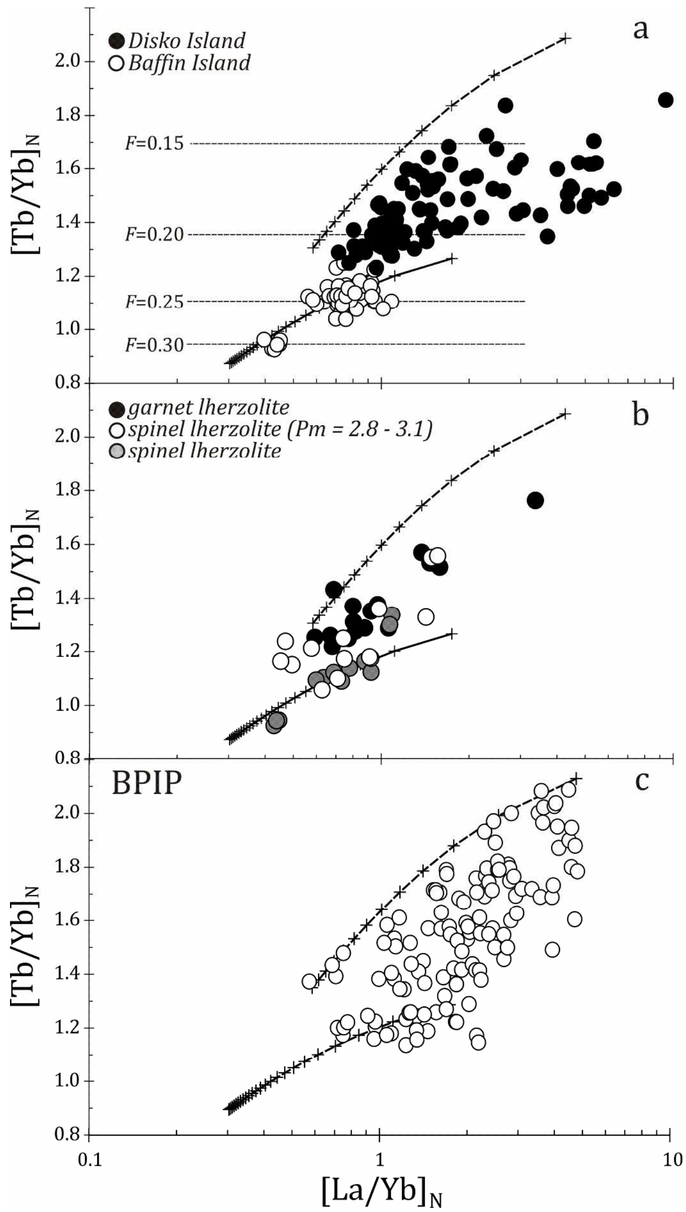

163x291mm (300 x 300 DPI)

Table 1. T_P, MgO and Mean melting column dimensions for NAIP primary magmas.

Location	Subgroup	*n*	MgO (wt %)	T_P °C	T_P °C range	P*i* (GPa)	P*f* (GPa)	*FAFM*	P*m* (GPa)
Faroe Islands Basalt Group		34	18.3±1.4	1519±36	1469-1551	3.9±0.6	2.4	0.23±0.06	2.8±0.4
Faroe-Shetland basin (217/15-1)		3	17.1-18.9	~1530	1510-1549	~4.0	3.1	~0.17	~3.2
East Greenland	<1500°C	5	15.6-16.3	~1460	1451-1468	~2.9	2.3	~0.20	~2.2
East Greenland	>1500°C	14	19.0±1.3	1539±34	1508-1553	4.3±0.7	1.8	0.28±0.10	2.3±0.8
BPIP	Whole rocks	45	17.7±2.6	1504±64	1451-1563	3.6±1.0	2.7	0.16±0.10	2.9±0.6
Mull Plateau Lava Formation melt inclusions		6	15.8-16.8	~1480	1455-1482				
Disko Island Vaigat Formation	T_P <1600°C	73	19.6±2.0	1548±32	1513-1581	4.6±1.2	2.8	0.21±0.08	3.5±1.1
Disko Island Vaigat Formation	T_P≥1600°C	7	21.7-23.0	~1620	1606-1639	5.9-7.0		≥0.3	> 3.5
Baffin Island Vaigat Formation		46	18.7±1.8	1532±48	1496-1557	4.2±1.0	2.1	0.26±0.06	2.8±0.8
Vaigat Formation melt inclusions (Baffin)		23	18.8±0.8	1533±22	1507-1551				
Iceland Rift Zones		57	17.8±1.4	1509±32	1475-1525	3.7±0.6	2.1	0.23±0.08	2.6±0.6
Iceland Rift flanks		20	15.7±1.0	1453±28	1423-1489	2.9±0.4	2.1	0.14±0.12	2.3±0.6